BIOFLUID LUBRICATION FOR ARTIFICIAL JOINTS

A Dissertation

by

ALICE MAE PENDLETON

Submitted to the Office of Graduate Studies of
Texas A&M University
in partial fulfillment of the requirements for the degree of

DOCTOR OF PHILOSOPHY

December 2008

Major Subject: Materials Science and Engineering

BIOFLUID LUBRICATION FOR ARTIFICIAL JOINTS

A Dissertation

by

ALICE MAE PENDLETON

Submitted to the Office of Graduate Studies of
Texas A&M University
in partial fulfillment of the requirements for the degree of

DOCTOR OF PHILOSOPHY

Approved by:

Chair of Committee,	Hong Liang
Committee Members,	Richard Grifffin,
	Jun Kameoka
	Christian Schwartz
Intercollegiate Faculty Chair,	Tahir Cagin

December 2008

Major Subject: Materials Science and Engineering

ABSTRACT

Biofluid Lubrication for Artificial Joints.

(December 2008)

Alice Mae Pendleton, B.S., Prairie View A&M University;

M.S., Rice University

Chair of Advisory Committee: Dr. Hong Liang

This research investigated biofluid lubrication related to artificial joints using tribological and rheological approaches. Biofluids studied here represent two categories of fluids, base fluids and nanostructured biofluids. Base fluids were studied through comparison of synthetic fluids (simulated body fluid and hyaluronic acid) as well as natural biofluids (from dogs, horses, and humans) in terms of viscosity and fluid shear stress. The nano-structured biofluids were formed using molecules having well-defined shapes. Understanding nano-structured biofluids leads to new ways of design and synthesis of biofluids that are beneficial for artificial joint performance.

Experimental approaches were utilized in the present research. This includes basic analysis of biofluids' property, such as viscosity, fluid shear stress, and shear rate using rheological experiments. Tribological investigation and surface characterization were conducted in order to understand effects of molecular and nanostructures on fluid lubrication. Workpiece surface structure and wear mechanisms were investigated using a

scanning electron microscope and a transmission electron microscope. The surface topography was examined using a profilometer.

The results demonstrated that with the adding of solid additives, such as crown ether or fullerene acted as rough as the other solids in the 3-body wear systems. In addition, the fullerene supplied low friction and low wear, which designates the lubrication purpose of this particular particle system.

This dissertation is constructed of six chapters. The first chapter is an introduction to body fluids, as mentioned earlier. After Chapter II, it examines the motivation and approach of the present research, Chapter III discusses the experimental approaches, including materials, experimental setup, and conditions. In Chapter IV, lubrication properties of various fluids are discussed. The tribological properties and performance nanostructured biofluids are discussed in Chapter V, followed by summary and conclusions in Chapter VI.

ACKNOWLEDGEMENTS

This dissertation would not have been possible without the help of many, especially my Lord and Savior Jesus Christ, whose words were implanted within my heart that I can do all things through Christ who strengthens me. Without the love, the support, the encouragement, and the patience of my husband, Rev. Dr. Walter Pendleton, this dissertation would not be possible. I thank my mother, Edna Jackson, who inspired me to be the best that I can in pursuing my dreams. I thank my brothers, Worley Flowers, Lorenzo Flowers, Charles Flowers Jr, Velton Flowers, and my sister, Abena "Lavern" Ajanaku, for their love and financial support. I thank my special friend, Odis Styers III, with a B.B.A. in Accounting from Texas A&M University from Hempstead, Texas for his encouragement and financial support.

In addition, I would like to express thanks to my advisor, Dr. Hong Liang, for her direction and encouragement during this work. I also would like to express appreciation to my Ph.D. committee members, Dr. Richard Griffin, Dr. Cris Schwartz, and Dr. Jun Kameoka, for their guidance and support. I would like to thank the members of the Liang Research Group who offered me their companionship and assistance. I express special appreciation and recognition to Dr. Prasenjit (Raj) Kar for his guidance and assistance to this project. Special thanks to Dr. Sahar El Houssamy, Dr. Subrata Kundu, and Lei Liu, who helped with the viscosity measurements.

Finally, I wish to acknowledge financial support from the NSF (grant number 0535578, including GRS fellowship).

TABLE OF CONTENTS

Page

CHAPTER Page

LIST OF FIGURES

FIGURE Page

FIGURE Page

FIGURE Page

.

LIST OF TABLES

CHAPTER I

INTRODUCTION OF BIOFLUIDS

This chapter concentrates on biofluids. There are two different kinds of biofluids: intracellular and extracellular. Of particular interest is synovial fluid, a type of extracellular fluid. In addition, this chapter discusses biotribology, which consists of lubrication of rigid surfaces, such as metals, ceramics, and polymers; and lubrication of soft surfaces, such as cartilage, cells, and rubber. Biotribology is discussed in terms of friction, which involves the Amonton's law of friction, abrasive and adhesive wear that occurs in joints and joint replacements. This chapter also discusses novel additives for lubrication, which are nanoparticles.

1.1 Body Fluids

All of the fluids in the human body are called body fluids [1]. Body water makes up about 62.5% of the intracellular compartment. Changes in the quantity of intracellular fluid (ICF) will affect one's health [1]. Extracellular fluid (ECF) makes up about 37.5% of the body water [1]. Extracellular fluids are fluids outside the cells, and intracellular fluids are fluids inside the cells [2]. The extracellular fluids are separated into numerous compartments, as follows [2]: The vascular compartment contains the blood plasma, which accounts for 7% of body water. Interstitial fluid accounts for approximately 18% of body water and is outside the blood vessels.

This dissertation follows the style of journal of Biomaterials.

After reviewing the body fluids, the body fluid of particular interest is the synovial fluid. The name synovial fluid comes from the word which refers to a gluey protein substance, an egg white like material that provides nourishment to muscular connections [3]. Synovial fluid (SF) is a viscous fluid found in hollow spaces of the joint [3]. Historically, SF was cited in the Greek Hippocratic text in "Of the Places of Man." It declares that there is a small amount of viscous fluid in the joints [4]. The quantity of synovial fluid in the human knee joint may be as little as 0.2 ml [5]. This fluid allows easy articulation of joints [4]. Another earlier historical account was by Galen, physician of Rome (AD 131-201) in "On the Function of Parts of the Human Body" [4]. It simply states that there is an oily body fluid on cartilage [4].

The SF is produced by the synovial membrane. SF fluid contains molecules that decrease friction and wear properties of the articulating cartilage [6]. The SF lubricates by providing proteoglycan 4 (PRG4), hyaluronic acid (HA), and surface active phospholipids (SAPL) [6]. PRG4, HA, and SAPL are produced by the synoviocytes of the synovial membrane and chondocytes in the cartilage in the synovial membrane [6]. Most recently, SF was defined as a blood plasma dialysate, which is composed of HA [7, 8].

Table 1: Molecules in Synovial Fluid.

Molecule	Concentration	References
Proteoglycan 4 (PRG4)	0.05-0.35 mg/ml	9, 10
Hyaluronan (HA)	1-4 mg/ml	11, 12
Surface-active phospholipids (SAPL)	0.1 mg/ml	12, 13

The molecules of SF are displayed in Table 1 [9-13].

SF is assumed to have two major functions. One function is to assist in the lubrication of the articulating surfaces [14]. Lubrication in the natural synovial joint is executed by utilization of synovial fluid, as indicated in Figure 1. The other function is to provide nutrition to the articulating surfaces [14]. The composition of SF changes due to the condition of the joint [14]. The protein substance changes depending on whether the joint is normal or diseased [14]. As a matter of fact, the protein amount in normal SF is much lower than plasma [15, 16]. The protein substances increased with diseased and/or inflamed SF [17, 18]. The SF contains HA in concentration of 0.14-0.4% [19].

For ten years [20], hyaluronan, previously named HA, had been the subject in Europe (Bayer) and other countries. The formula for HA was developed for intravenous usage in horses in the United States by Bayer Pharmaceuticals, and was approved and

promoted in Europe (Bayer) and other countries [20]. The potency of HA was modified for the joint type of individuals [20]. The smaller joints displayed a higher application of HA [20]. HA is a critical ingredient of SF and the articular cartilage in normal diaarthrodial joints [20].

Several reports have connected molecular weight with lubricants that contain HA. These reports demonstrate that the lubricant functioning of HA improves with rising molecular weight [21-25]. This improvement of lubricant performance was probably because of the increase in viscosity with increased molecular weight [22]. It Yokabori et al. [26] pictured the utilization of watery HA solutions as an artificial SF. It was pictured where articular cartilage was missing. It was also evaluated as an artificial SF [26]. This was done many times with sliding samples compiled of metal and articular bone without cartilage [26]. The viscosity of HA 1900 and HA 1800 were measured in this work [26]. The viscosity of HA1900 was approximately four times greater than HA1800 [26]. was proposed in this study [26] that HA of higher molecular weight was useful in treatment of cases where the artificial cartilage was missing.

The composition of normal, osteoarthritis (OA), and rheumatoid arthritis (RA) SF is displayed in Table 2 [27-32]. When there is asperity against asperity contact, it results in mixed lubrication [31]. In mixed lubrication, the load is carried by the contact of the asperities along with the load from the lubricant [31]. With mixed lubrication, the bearing surface irregularities will happen along with different areas of the sliding surfaces, as indicated [31] in Figure 2, top view. Fluid film lubrication occurs when the lubricants have complete separation of the bearing surfaces [31]. When the two surfaces

make a film, it will create a separation to keep the two uneven surfaces away from each other [31]. This result of fluid film lubrication will occur, and the asperities will pass each other without contacting [31]. This will cause reduced friction and wear. If there is contact between the articulating surfaces of the bearing, increased friction and wear will result [31].

Table 2: Revised Composition of Normal, Osteoarthritis (OA), and Rheumatoid Arthritis (RA) Synovial Fluid [4].

Substance	Normal		OA		RA	
	Amount	Ref	Amount	Ref	Amount	Ref
HA Mw (MDa)	6.3-7.6	[27]	1.06-3.4	[32]	3.2-3.6	[27]
HA (mg/ml)	2.50-3.65	[28]	1.07-2.60	[28]	0.39-2.19	[28]
Protein (mg/ml)	10.4-15.8	[29]	17.0-56.8	[30]	31.6-66.2	[30]
Phospholipid (mg/ml)	0.13-0.15	[31]	0.26-0.98	[31]	0.40-1.40	[31]
Total Choles. (mg/ml)	0.07-0.08	[31]	0.04-1.69	[31]	0.76-1.30	[31]
Triglycerides (mg/ml)	0.12-0.59	[31]	0.17-1.00	[31]		

1.2 Biotribology

Biotribology is the knowledge of tribology as relating to the performance of biological functions [33]. It applies to synovial joints and their replacements. This branch is involved with the movement of both natural and artificial bearing systems using loads. [33]. It is comprised of three areas as follows: lubrication, friction, and wear.

In the natural human joint during lubrication, the same principle applies. The frictional patterns of bearing are adapted by the existence of a lubricant [33]. The performance of the lubricant on the bearing depends on a number of factors. These

factors are viscosity of the lubricant, features of the surfaces, and roughness of the materials. A critical factor in determining the lubrication regime is the roughness of the material [33]. Roughness is the asperities of the surface with peaks and valleys [33]. There are basically two kinds of lubrication. They are boundary lubrication and fluid film lubrication. With the lubricant, the bearing can operate in one of theses mechanisms: boundary, mixed and full film lubrication as indicated in Figure 2. Fluid lubrication is lessening friction by providing a film of fluid between the articulating surfaces [34].

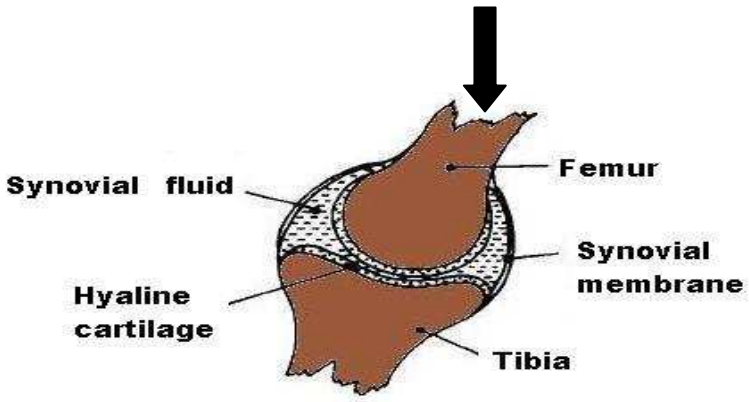

Fig. 1: Diagram of Synovial Joint [36].

Boundary lubrication is said to occur when the bearing surfaces are only partially separated by a lubricant [35]. In this type, the load is carried by the asperities, although a lubricant may be present. Sometimes there is no lubricant, and this mode is known as dry regime. The fluid is under pressure in the bone tissue and between the surfaces [35]. It can bear major portions of the load. The determination of load bearing happens within

the molecules of the film at the articular cartilage [35]. This occurs at the asperity-to-asperity contact in the boundary lubrication.

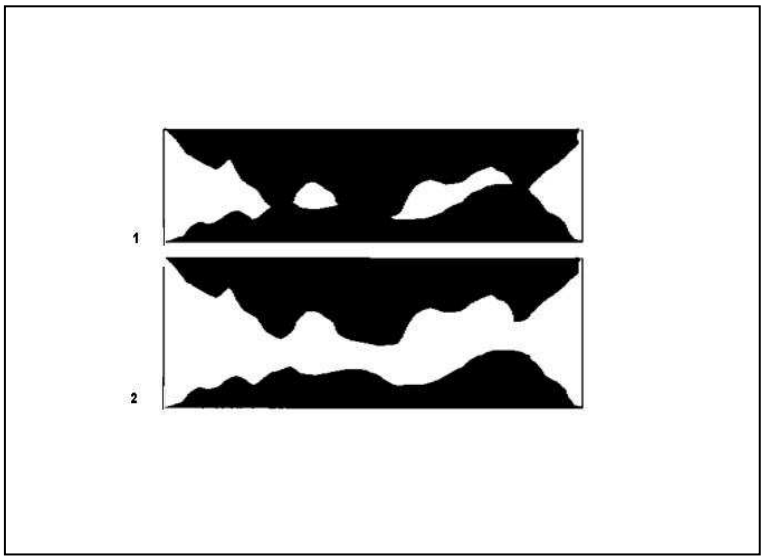

Fig. 2: Mixed and Full Film Lubrication. (1) Mixed Lubrication Consists of Full Fluid Film and Boundary Lubrication (2) Full Film Lubrication Mixed and Full Film Lubrication [31].

In this mixed lubrication mechanism, there is an intermediate between boundary and fluid film lubrication [35]. The term fluid film needs additional interpretation, for the connection can function as lubrication regimes such as hydrodynamic or hydrostatic lubrication [35]. In the hydrodynamic bearing, the lubricant is drawn into a channel of decreasing height by the surface motion of the solids [35]. The Couette flow rate or surface velocity at any section reducing as the canal becomes slender [35]. This necessitates the opening of another flow action named Poiseuille or pressure flow maintaining the management of mass flow [35].

1.2.1 Lubrication of Rigid Surfaces

The rigid surface is defined as a surface lacking flexibility. In medical devices, materials were first described as not living for biological applications [37]. Later, biomaterial was indentified by Black as natural material to replace living tissues [38]. The twofold main concerns of new bone materials are mechanical properties and biocompatibility [39]. It is a well-known fact that the mechanical properties of biomaterials have been well distinguished [39]. The common criteria for material selection for bone implant materials are that they must be highly biocompatible [38]. They must cause a toxic response within acceptable limits [39]. They must have suitable mechanical properties close to bone [39], as shown in Table 3 [39-41]. The last criterion is that the materials and manufacturing process must be economically feasible for usage in lubrication [39]. Rigid surfaces such as metals, ceramics, and polymers have been investigated for artificial joint materials. These rigid surfaces apply to materials that have high elastic modulus.

Table 3: Mechanical Properties of Bones [39-41].

Hard tissues	Compressive strength (MPa)	Tensile strength (MPa)	Elastic mod. (GPa)
Tibia	159	140	18.1
Femur	167	121	17.2
Radius	114	149	8.6
Humerus	132	130	17.2
Cervical	10	3.1	0.23
Lumbar	5	3.7	0.16

A. Metals

For centuries, there have been efforts to develop biomaterials for joint replacements for diseased and injured human joints [39]. While there are unsafe ions discharged form these alloys, they are still used for their mechanical properties [39]. In the beginning, femoral mechanisms of THR were composed of stainless steel [39]. Metal alloys have been the main material utilized for lubrication due to their unique automatic features [40]. Later on, they were replaced with cobalt chromium molybdenum [41, 42].

Table 4: Revised Mechanical Properties of Alloys in TJR [40, 46].

Alloy	Ten. force (MPa)	Mod. (GPa)
Pure titanium	785	105
Ti–Zr	900	
Co–Cr alloys	655–1896	210–253
Co–Cr–Mo	600–1795	200–230
Ti–6Al–4V	960–970	110

The metal-on-metal mixture utilizing cobalt–chrome alloys was recently introduced again as the bearing pair for artificial hip joints [43]. This occurred after the long-term achievement of some earlier McKee-Farrar implants [43]. In addition, the parameter that has gotten less attention is femoral head radius [43]. Most of the metal-on-metal hip prostheses use a 28 mm diameter radius. It was duplicated from ultra-high molecular weight polyethylene (UHMWPE) on-metal arrangement [43]. Nevertheless, most recently, a larger radius of the femoral head has been investigated [43].This work established that an increase in femoral head radius is also capable of escalating the wear under boundary lubrication [43]. This tendency can be inverted to a mixed lubrication in the direction of fluid film lubrication [43].]. It has been determined that the clearance between the femoral head and the acetabular cup are significant [44, 45]. In Table 4 [40, 46], are listed the general mechanical properties of metallic alloys utilized in total joint replacement (TJR).

B. Polymers

Orthopedic devices such used in THR are polymers with high strength and stiffness as needed [39]. Orthopedic biomaterials that are in widespread usage because of their properties are polymers [39]. Escalating the crystalline of polyethylene (PE) initiates an enlargement of the PEs' modulus of elasticity ensuing in more intense contact stresses [47]. But if the contact stresses are not uniformly isolated, the wear rate of the PE will increase [48]. The widespread polymers for orthopedic usage are: UHMWPE and propolylene (PP) [49]. Safe and sound polymer systems such as polytetrafluoroethene (PTFE), UHMWPE, or poly (etherketone) PEEK have been studied due to their outstanding mechanical properties [39]. As stated earlier, in the early 1960s, the stainless steel femoral THR component was partnered with PTFE acetabular cups [39]. The stainless steel as well is stiff and could not be utilized for THR. Yet, it was determined by Wang et al. [50] that fluid film lubricants were not successful in lubricating the metal partnered with PE joints. The findings showed that less clearance led to a low coefficient of friction under a changeable loading and that was often associated with less wear [50]. Polymers displayed in Table 5 [51, 52] indicate the mechanical properties.

Table 5: Revised Mechanical Properties of Polymers Used in THR [51, 52].

Material	UCS (MPa)	UTS (MPa)	Modulus (GPa)
Polymers			
HDPE	25	40	1.8
UHMWPE	28	21	1
PE	35		0.88
PEEK	139	8.3	
PTFE	11.7	28	0.4
PMMA	144	21	4.5

C. Ceramics

Ceramics have been used as a substitute for the metal alloy with polymer bearing. An example of one of these alloys is CoCr-UHMWPE bearing pair, which was utilized in total hip arthroplasty (THA) [53-55]. In addition, it was also used in total knee arthroplasty (TKA) [56-58]. The most commonly used ceramic in THA is Al_2O_3 [57]. The THA and TKA were utilized for many decades. In the 1970s, Alumina (Al_2O_3) was pioneered as a contender material for orthopedic bearings, but this material was too brittle [59]. The restriction of ceramic surfaces in orthopedic applications is correlated to their weakness [59]. This can lead to catastrophic failure in vivo [59]. The benefit of ceramic surfaces in artificial hip and knee joints is the critical decrease in wear percentage of the bearings [60]. Recent ceramic bearings are safe, sound, and reliable when used with THA and TKA components. The total hip replacement (THR) must

display the mechanical properties as indicated in Table 6. They have a verified plan, and their progress is examined to decrease the danger of ceramic bearing breakdown [60].

Table 6: Mechanical Properties of Ceramics Used in THR [51, 52].

Ceramic	UCS (MPa)	UTS (MPa)	MOD (GPa)
Zirconia	2000	820	220
Alumina	4000	300	380
Bioglass	1000		75
C—(Graphite)		138	25
C—(Vitreous)		172	31
HAP	600	50	117
C—(LTI pyrolitic)	900	28	

1.2.2 Lubrication of Soft Surfaces

This section focuses on materials that have low elasticity or surfaces covered by dangling bonds or soft coatings. There is a center on the elastohydrodynamics of soft boundaries [59]. Stimulated by many functions in physical chemistry, polymer physics, the process is biological lubrication [61]. An amount of work concentrates in these areas on problems such as cartilage biomechanics [62-64]. Other reports concentrated on the motion of red blood cells in capillaries [65-73], elastohydrodynamics of elastomers [74, 75], polymer brushes [76,77], vesicles [78,79], and among others.

This is extremely low and is similar to the hydrodynamically lubricated bearings [80, 81]. Several natural surfaces display interesting low friction properties [80-89]. Case in point, cartilages of animal joints include a friction coefficient in the span of 0.001–0.03 [89].

1.2.3 Friction

Mutually, the frictional behavior of natural and artificial joints has not been paid enough attention [31]. Friction is the rubbing of one surface against another. Amonton, developed the laws of friction, and declared that the frictional force (F_f) formed is relative to the load (F_n in N) rubbed across the bearing surfaces [31]. This formula is denoted as FμN, where μ is the coefficient of friction, as indicated in Figure 3. The frictional force is free from serving the contact area.

$\mu = Ff/Fn$ Friction Coefficient……..……... (1)

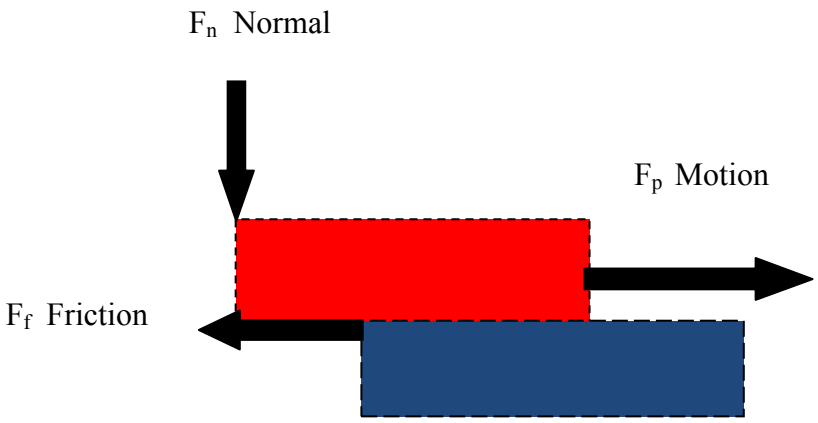

Fn: Normal load, Ff: Friction load, Fp: Applied load

Fig. 3: Normal and Friction Force in Relation to Bearing Surfaces.

1.2.4 Wear

Typical wear may be defined as volume or mass loss caused by articulating or sliding of two surface materials [32]. Wear is the detachment of material from rubbing surfaces in a relative motion. There are two basic types of wear mechanisms, abrasive wear and adhesive wear [32]. Although wear of artificial joints can happens primarily at the articulating surface, it can also happen at the interface of the joint. For example, the interface of the narrow part of the femoral constituent on the perimeter of the cup may also cause polymeric debris. To a first approximation, the amount of volumetric wear, V, generated in either mixed or boundary lubrication regime can be determined from the following equation [33]:

Wear volume (V) = wear factor (k) x load (N) x sliding distance (m) ……. (2)

During the articulation of joints, the wear of artificial joints happens at the surface or the interface of the joint. Wear volume can be established by this equation [33]. The units for wear volume are V = Nm. The volume of material detached from the bearing surfaces is defined as wear volume. The amount of wear volume is denoted by the letter (V) and is produced in either mixed or boundary lubrication regime [33]. The wear factor value relies on the state of the bearing contact as well as the materials utilized along with surface irregularities [33]. These are two of the main forms of wear are indicated in Figure 4. Abrasive wear is a plowing of hard fragments from surface produces reduction of fragments from the contacted surfaces. Adhesive wear is where fragments from the contacted surface lodges to another surface and are torn off due to the sliding motion.

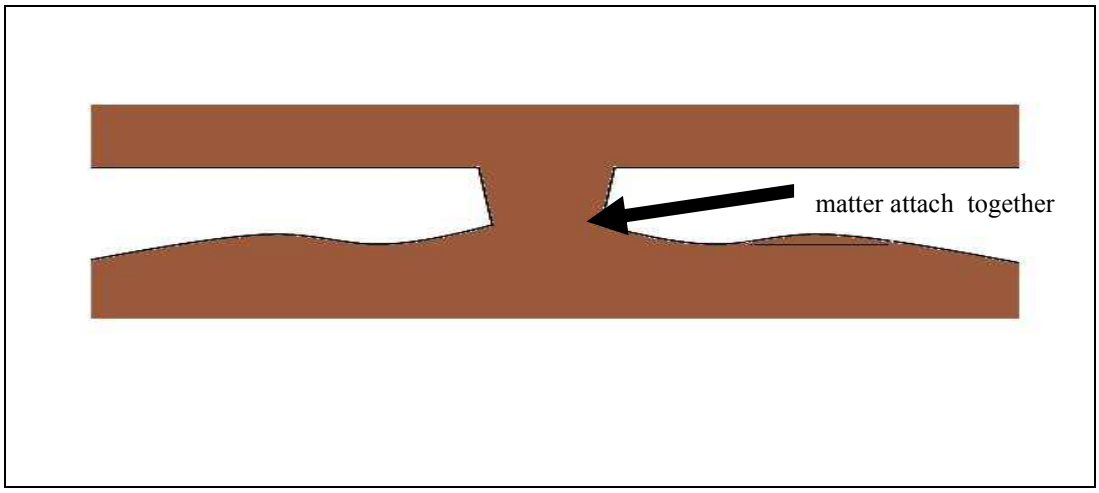

Adhesive Wear

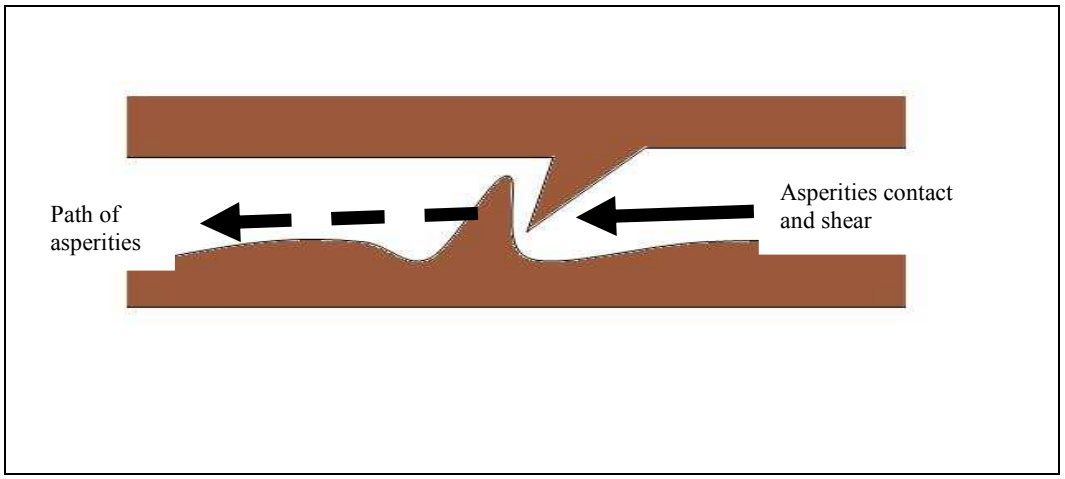

Abrasion Wear

Fig. 4: Diagram of Forms of Wear

1.3 Arthritis

Arthritis is a collection of diseases that destroy the joint and/or articular cartilage [90]. There are several forms of arthritis, but of significance in this research is osteoarthritis (OA). More than 20 million people are bothered in the United States with OA [91]. In doing so, the bone becomes fragile cannot handle the load of the joints, and the outcome is pain [92]. Healthy articular cartilage can handle huge forces due to weight and joint movement [93]. With OA, there is cartilage degeneration [93-95]. As a result, there are cracks, partial or complete loss of bone tissue [93-95]. The end of the bone is covered with a slippery surface named cartilage [96]. OA is a joint disease characterized by the wearing away of the articular cartilage [96].

Healthy cartilage, as referred to earlier, allows the bones to glide over one another. It also absorbs the shock of movement [96]. In OA, the cartilage surface layers begin to deteriorate and eventually collapse. When this happens, it allows the pressure and friction to bones directly. This causes pain and swelling, which eventually ends in no movement of the joint. A regular place where OA occurs is the hip joint, which is the most significant weight-bearing joint in the body [97].

1.3.1 Injections for Osteoarthritis

Intra-articular corticosteroids have been used to handle arthritic conditions since the beginning of the 1950s [98]. Researchers explained that intra-articular hydrocortisone reduces the leukocytes count, along with the temperature of the synovial fluid [99]. In addition to the use of cortisteroid injections, the use of anesthetic injections to control pain from an arthritic hip has been advocated for many years [99]. An

injection of cortisteroids and local anesthetic into a hip joint has been shown to produce short-term improvement in hip pain but has not produced long-term improvements in patients' symptoms [100]. The hip injection also has been used in patients for whom there is a long delay prior to hip replacement surgery, as well as for those who are not in good physical condition [101].

Concern has been raised recently that the use of intra-articular steroids can contribute to the development of infection. It happens normally following the injection, but in the longer term, it influences the outcome of total hip replacement [99]. Results indicate that 128 patients had hip joint injections and underwent successful total hip replacement [102]. Afterwards, there was no evidence of associated risk of prosthetic infection. There was also no risk following revision of total hip arthroplasty. When the hip infection occurs normally 3.2 years after injection with cortisteroids [102], the only conclusion was that hip injection was safe if a strict aseptic procedure is maintained [102]. The time period of pain relief with hip injection is limited to an average of 2 months [102]. For analytical intent injections, using local anesthetics is suggested [102].

1.4 Joint and Joint Replacement

A joint describe the area where two or more bones meet and produce movement [103]. Fibrous joints are bones joined by tissues having fibers [103]. Bones joined by hyaline cartilage are called cartilaginous joints [103]. Synovial joints contain joint cavity surrounded by a capsule, and it is surrounded by a synovial membrane [103]. The skeleton structure bones are connected by fibrous, cartilaginous, or synovial joints [104]. Synovial joints are organized into six kinds due to the types of their movement [104].

The following joints are planar, hinge, condylar, sellar, spheroidal and polyaxial, as described below [104]:

- Planar joints like the carpals of the wrist are the simple joints that move back and forth and side to side.
- Hinge joints, such as the elbow, allow bending.
- Condylar joints like the wrist allow flexion/extension and rotation.
- Sellar joints resemble sadddle are the base of the thumb movement.
- Spheroidal joints allow movements in many directions.
- Polyaxis joints allow unrestricted motion, such as in the hip and shoulder.

Historically, joint replacement began with Smith-Petersen in 1930 when he inserted a plastic cup between bone ends [105]. It was later made of stainless steel and chrome-cobalt alloy. Later in 1940, the first artificial hip joint was made in Norwich [105], because there was a problem with the acetabular cup attachment. The attachment problems were solved by using a lag screw to fuse the hip [105]. This artificial hip was utilized three times in 1950. The British Orthopedics Association (BOA) verified the artificial hip in 1951 [105]. Two artificial joints were made from stainless steel, but the screw came loose and the joint malfunctioned in a year [105]. The third type was attached with chrome-cobalt screws in a 70-year-old woman, and it was victorious for three years [105].

Charnley made an effort to restore the acetabular socket with polyethylene in the 1960s [106]. It was successful because of the usage of polyethylene as articulating material in joint replacements [106]. It is still commonly utilized today. Artificial joints

have been used for over 100 years [106]. However, in the past 50 years, there has been some outstanding progress. The Charnley low resistance arthroplasty was one of the most notable artificial joints [106]. The original type integrated a stainless steel femoral head articulating against PFTE acetabular cup [106]. Although the artificial joint was low friction, the wear of PTFE was extremely high. Therefore, the PTFE was replaced with UHMWPE as the cup material [106].Currently, the ultra high molecular weight polymer ethylene (UHMWPE) is being used as a bearing material. It is used because of its biocompatilbity and good wear resistance [107]. The wear rate of UHMWPE is small compared to other plastics. However, it is still large enough to produce problems that cause a biological response and eventually implant failure [107]. TJR is when a diseased or injured joint is replaced with a biocompatible synthetic material.

In a recent study, 2000 Charnley joints [108] provided over 77% of patients, and they are still functioning well after 25 years.

The main reason for TJR is arthritis [109]. Two articulating surfaces are a metal ball, called the femoral head and stem, and an UHMWPE liner [109].The common view of a TJR consists of an acetabular cup, femoral ball, and stem to establish the articulating effect [110-112]. The schematic of a THR is displayed in Figure 5. The part that interfaces with the bone is usually made of a metal alloy.

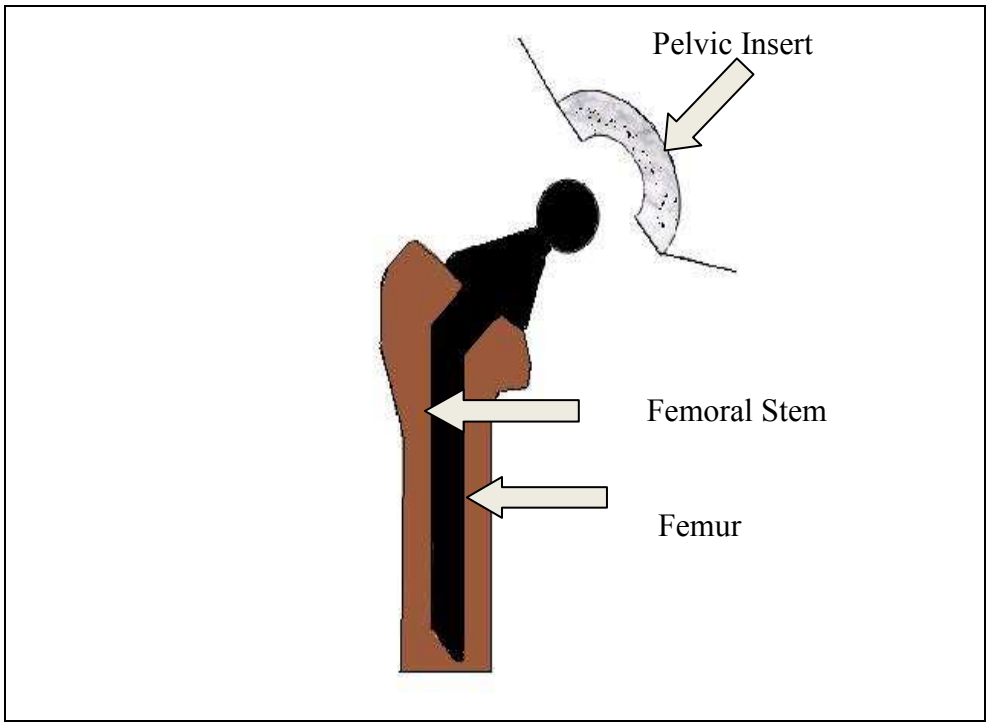

Fig.5: Total Hip Replacement.

1.5 Nanoparticles

The combination of biology and materials at the nanoscale has a prospective for transforming numerous disciplines, such as science and technology [113]. The nanometer size scale is important in biology. It is significant because of the measurement of large biomolecules, such as proteins and DNA. It is important for other cellular formations descended in 1-1000 nm spans [113]. In the past, nanostructured materials were mainly limited to circular particles of gold and silver [113]. In recent times, a wide selection of nanomaterials has been combined and utilized for biological applications [113]. Marketable spherical magnetic beads are used for cell separations [114, 115], quantum dots are used for fluorescence examination in cells [116], and

colloid gold is used for gene therapy [113]. More difficult particles are a potential for connections to biological molecules [113].

These materials frequently have innate chemical, electrical, magnetic, and optical anisotropy properties [113]. They can correlate with cells and biomolecules in a basically novel behavior [113]. Current developments in nanomaterials production have been focused on a combination of high aspect ratio particles at nanometer length and time-span scales [113]. Their structures can be elongated. The exclusive and highly developed properties are natural to bare nanoparticles of metals as well as semiconductor complexes [117-120].

Silica is a dioxide of silicon (SiO_2). Silicon nanopartilces are yellowish to reddish-brown in color. Silicon is composed of small particles in sizes between 8 and 200 nm, as seen by transmission electron microscopy (TEM) [121]. In the electron micrograph, the particles are clustered in black up to 162 $m^2 g^{-1}$ [122]. SiO_2, a chemical compound, has been recognized for its hardness since the 9th century [123]. As with most nanomaterials, clusters of SiO_2 nanoparticles have been the greatest problem in their broad applications [124, 125]. The qualities of nanoparticles are hardly in usage because they are usually dispersed in medium of micro dimension [126, 127]. Concentration is now in the direction of silane coupling driving force. In this work [128], silane coupling agents made nano-SiO_2 disperse fine and gradually in numerous organic mediums. The structure of nano-SiO_2 was portrayed by TEM [128]. It was described by infrared spectrum (IR), X-ray photoelectron spectra (XPS), and thermogravimetric analysis (TG) [128]. The dispertivity of nano-SiO_2 was calculated by

light transmittance (LT). The tribological properties of opposing wear and friction reduction were evaluated by RFT-III Reciprocating Tribotester [128]. In addition, it was evaluated by MS-800 four balls Tribotester [128].

These particles illustrate better dispertivity in several organic solvents, such as diesel oil, liquid paraffin, and CC_{l4} [128]. After observing the nano-SiO_2 small particle size and greater dispertivity in lubricants, an investigation of their tribological performance utilized as additives was completed. As anticipated, these nanoparticles can be fixed into the micro-cracks on the surface of friction pairs to prevent the cracks from additionally increasing [128]. The determination was made that modifiers such as KH-550, KH-560, and KH-750 were used as silane agents' pairing by way of surface revision in situ [128]. The outcome demonstrates that these modifiers are shared by the surface of nano-SiO_2 by covalent bonds and revise the surface properties of nano-SiO_2 [128]. These nanoparticles have better dispertivity and strength in various types of organic solvents [128]. The tribological study of these particles as additives in lubricants will disclose their prospective in lubrication [128].

Zinc is a metallic chemical element with the symbol Zn and atomic number 30 on the periodic table. Zinc oxide formula is ZnO and is a compound formed by the oxidation of Zinc. In this work [129], the authors investigated the anti-wear (AW) and extreme pressure (EP) properties of ZnO nanoparticles as additives in a polyalphaolefin (PAO6) [129]. In addition, the influence of dispersing agents in the overall tribological behavior was investigated [129]. The main properties of the nanoparticles are the lubricant and dispersing agents used are listed in Table 7.

Table 7: Material Properties of Nanoparticles, Lubricant, and Dispersing Agents [129].

Nanoparticles: ZnO	Properties: Morphology: nearly spherical, purity: 99.5%, size: 20 nm
Lubricant: PAO6	Physical properties: Density (15.6oC): 0.826 g/cm3, Viscosity: 31.0 cSt (40^{o}C), 5.90 cSt (100^{o}C), VI: 135
Dispersing agents	Description Commercial name: Octacare ® DSP-OL100 Density: 0.91 g/cm3, Character: non ionic
OL300	Commercial name: Octacare ® DSP-OL300 Density: 0.90 g/cm3, Character: non ionic
Test balls	Chemical composition: 0.98-1.1% C, 0.15-0.30% Si, 0.25-0.45%Mn, 1.30-1.60% Cr, <0.025% P, <0.025% S

The dispersing agents OL300 and OL100 assumed an anti-wear agent when they were annexed to PAO6 [129]. The elemental analysis illustrated that dispersing agents did not react chemically with the metallic surface [129]. Esters tend to move to metal surfaces and create bonds with the surface oxides layers, although they are polar molecules [129]. There is a probability of usage as friction reducing additives in low polarity base oils such as PAO along with mineral oils [130-133].

The following conclusions were drawn from the results of this study [129]: Two esters, OL100 and OL300, were used as dispersing agents. A stability study by sedimentation showed that clusters were created at all OL100 concentrations. The stability study displays creation of clusters for 1 and 1.5% of ZnO in PAO6+3% OL300 [129].

ZnO particles do not function as an anti-wear agent under certain conditions. EP performance gets better when the PAO6+1% OL300+ZnO mixtures are correlated to the enhancement of ZnO nanoparticle dilution [129]. These compounds PAO6+3%+ OL300 ZnO displayed the best EP functioning in PAO6+3% OL300+1% mixtures [129]. PAO6+3% OL300+1% ZnO and PAO6+3% OL300+3% ZnO displayed an inferior result in spite of ZN nature [129]. In addition, the tribological functioning of ZnO nanoparticles were researched with an additive such as polyalphaolefin (PAO_6) [129].

Another nanoparticle under consideration is Palladium (Pd) nanoparticles [134]. Pd is a transition material, and it is a noble metal. The noble characters of these metals prevent the oxidation processes [134]. The defense mechanism continues as long as the substrate is not accomplished [134]. The use of noble nanoparticles for these functions could be a hopeful objective [134].

Other noble metals, along with Pd, , gold, and silver have been used as protective lubricant materials in the form of alloys [135], coatings, or multilayer's for electrical contacts [136, 137]. The major outcome is a sharp increase in the contact resistance, whose outcome was a fault of the electronic devices linked via contact [138].

This work describes for the first time the service of surface-modified Pd nanoparticles with a regular size of 2 nm additives for lubricant oils [134]. The alklyammonium surface chains in mixture with their nanometer size may conform to the demands of good dispersion and improvement of tribological properties [134]. The 5 wt% nanoparticle dispersions of tribological performance is explored and compared in terms of friction and wear to the base oil only [134]. The modifications of the electrical properties of the contact area were done due to the metallic nature of the nanoparticle center [134].

Alumina oxide (Al_2O_3) is a ceramic. It is formed by the oxidation of aluminum. It is used to enclose melting metal in applications where the material must function at high temperatures. It is also used where high strength is required [139]. In addition, it is used for electronic packaging that shelters silicon chips [139]. One traditional application is usage for insulators in spark plugs. Another sole application is established in dental and medical utilization [139].

The authors considered the methods dependable for the third body improvement of nanoparticles Al_2O_3 [140]. It also reduced friction in case of alumina ball sliding adjacent to a 316L stainless steel plate [140]. This attempt was intended to make clear the procedures accountable for the third body structure in Al_2O_3 nanoparticles in aqueous suspension [140]. The coefficient of friction of these nanoparticles Al_2O_3 were lessened about 40-50%, and the metal wear rate performed just as well [140]. The Al_2O_3 nanoparticles of micrometer size obtained a reduced effect of the lubricant [140]. When evaluated by the suspension of Al_2O_3 at pH 11, the particles clustered into bigger

particles [140]. This presented comparable outcomes in terms of wear, but at a higher friction coefficient [140]. Probably in both cases, a third body layer was created. Nevertheless, its formation and/or its depth were less competent in defending the metal than the coating formed by nanopartilces in the established suspension [140]. These researchers discovered that [141] the existence of Al_2O_3 nanoparticles of 150 nm diameter in an aqueous suspension lessened the degree of metal loss.

Many applications utilize nanostructural materials. These applications include catalysis, sensors, and molecular electronics [142, 143]. The research of organic-inorganic composite nanopartilcles is producing interest in science and industry [144, 145]. The use of inorganic nanoparticles tribology in recent years has received an abundance of attention [144, 145]. This awareness is producing more attention as a lubrication material [146, 147]. Still, they are chiefly used as polymer fillers and/or lubricating grease additives [146, 147]. Some fluorides, such as calcium fluoride (CaF_2), cerium fluoride (CeF_3), and lanthanum fluoride (LaF_3), have opposing wear ability [148-153]. The TiO_2 nanoparticles can advance the tribological properties of the base oil [154, 155]. The F atom has a small radius, and the tetrafluorbenzoic acid (FA) has a compact structure, which contributes to antioxidant, anticorrosion, and antiwear properties [156]. In this effort [156], the FA, C_6HF_4COOH, and surface modified TiO_2 nanoparticles were produced using sol-gel technique. The tribological properties in liquid paraffin were investigated utilizing a four ball tester. The outcomes show that the FA-TiO_2 nanoparticles exhibit good function in wear and friction reduction [156]. Investigation of the rare earth halides as solid lubricants has been accounted in current years.

The work [157] has investigated the tribological properties of LaF_3. The author states that the anti-wear property of bonded coatings could be enhanced by two or more times [157]. Another work [158] has reported CeF_3 and ceramic oxide (CeO_2) as solid lubricants that had anti-wear and friction-reduction properties at high temperatures. CeF_3 nanoparticles were tested by [159] and [160] as a grease additive. The investigation of CeF_3 nanoparticles additives in oils has not been described until present [161].

The authors [161] have projected the method of the synergism between CeF_3 and zinc dialkykdithiphosphate (ZDDP) in lithium grease. When CeF_3 was distributed in barium complex soap grease, the first seizure load was higher than when only Molybdenum Disulfide (MoS_2) was added [162]. They believe that ZDDP could restrain the decay of CeF_3. The physical content of CeF_3 nanoparticles indicates that their colors are white [162]. In this physical behavior, the size is about 25 nm, and their shapes are spherical and cylinder, as indicated in this work [162]. These results are summarized below [162]. The micro-emulsion of T154/cycloheplaedxane/water can be utilized to produce mono-dispersive CeF_3 nanoparticles [162]. CeF_3 nanopartilces displayed excellent extreme pressure and friction reducing properties [162]. The greatest non-seizure load (PB) assessment is inflated by 85.3%. The diminishing percentage of friction coefficient is greater than 25%, as contrasted with background oil [162]. In comparison, the anti-wear property of CeF_3 nanoparticles is deprived, and the wear scar diameter is reduced slightly [162]. The development of a transfer film in contact surfaces may be accountable for the outstanding tribological properties of the oils, including CeF_3 nanoparticles [162]. In conclusion, the cause of poor opposing wear properties of these

nanoparticles may be caused by the F- ion structure, which causes these F- ions to corrode the contact section [162]. The effects of nanoparticles on lubricants are displayed in Table 8.

Table 8: Summary of Effects of Nanoparticles on Lubricants.

Nanoparticles	Effects	Reference
SiO_2	Improve dispersion in oil	128
ZnO	Anti-wear problems	129
Pd	Low wear	134
Al_2O_3	Lower friction and wear	139
TiO_2	Reduced friction and wear	156
CeF_3	Poor wear	162

CHAPTER II

MOTIVATION AND APPROACH

2.1 Improve Lubrication of Artificial Joints

The result of inadequate lubrication of artificial joints is the major concentration of this research. At this time, the artificial joint is not lubricated sufficiently. The artificial joint with insufficient lubrication causes persistent pain and the patient is not able to move easily. One of the main reasons for artificial joint failure is inadequate lubrication. During articulation of the artificial joint, there is increase heat which leads to damage of the acetabular cup. Insufficient lubrication will result in persistent pain to the patient who receives the implant or revision of implant.

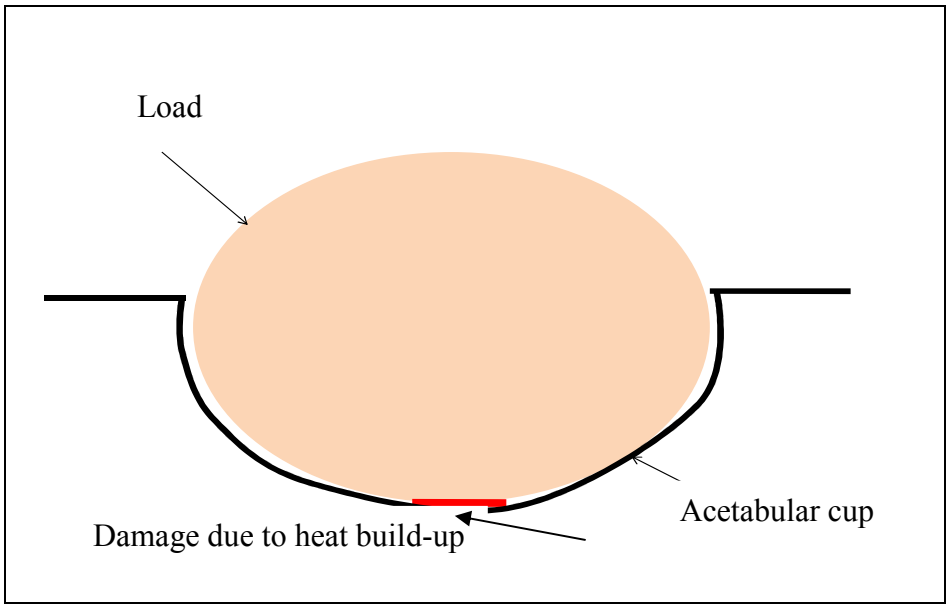

Fig. 6: Insufficient Lubrication of Artificial Joint.

Currently, prostheses are prepared with artificial materials, including titanium and titanium alloy. The major drawbacks in using these synthetic materials are they encounter degradation after many years of service. The joint eventually fail sometimes because of inadequate lubrication. The major motives for using titanium alloys are that they are strong and resist corrosion. Another motive is they have elastic modulus of about 105-110 GPa which is near the elastic modulus of bone. An additional motive is they are compatible with the human body, but the biocompatibility is not the present focus of this work.

2.2 Development of Nanostructured Biofluid

There are several biofluids, but the one of particular interests is the synovial fluid. Many researchers have tried to emulate the lesser wear and lesser friction of the synovial fluid but were unsuccessful. Many biofluids are presently in usage for lessening pain in diseased and artificial joints. Many provide immediate relief, but they only last for a short length of time. Nanofluid such as water and fullerene display lesser wear and lesser friction.

2.3 Research Objectives

Due to the insufficient lubrication of artificial joints, there is an immediate need to develop a lubrication-utilizing nanostructured biofluids. These biofluids would boost the length of usage and upgrading of the artificial joint.

Disease and injury many times cause joint replacement. One of the breakdowns of joint replacement is insufficient lubrication. This occurs during the articulation of

the joint, there is increased heat and which leads to wear. It is essential to reduce the friction and wear rate of lubricating biofluids that cause damage as indicated in Figure 6.

There is a necessity to improve the lubrication of the artificial joint. Novel biofluids for lubrication help the joints last longer. Currently, only biofluids exist to ease the pain of arthritic and/or artificial joints, but they have disadvantages. Inadequate lubrication may be the reason patients have joint stiffness and pain with barometric pressure due to the weather change. It was, therefore, proposed that this research would do the following:

- Investigate tribological distinctiveness of nano-structured biofluids for possible synthetic joint lubrication with present metals used in joint replacement.
- Examine the likelihood of evolving a nanostructured biofluid that would enhance the lubrication of synthetic joints.
- Expand a method to formulate nanostructured biofluids that are appropriate to biotribological purposes. .

2.4 Approach

The biofluids examined in this investigation are separated into two types: support fluids and nanofluids. The support fluids were water, simulated body fluid (SBF), and synthetic fluid [SBF + hyaluronic acid (HA)]. The nanofluid solutions utilized were [water fullerene (FU)], [water + crown ether (CE)] for contrast, [water+hydroxylated fullerene (FUH)], bovine, bovine fullerene, and bovine+hydroxlated fullerene.

Materials for control and contrast:

- Alumina (improved used in joint prostheses)
- Tititanium (dental implants)
- Ti-6A-l4V alloy (joint prostheses)

The information on the motivation for choice of materials and data on their features are provided in Chapter III. The techniques recognized for characterization of selected nanofluids and their contrast with the control materials were supplied in Chapter IV. Tribological and rheological features were performed and evaluated. The required features were lesser friction, lesser response, and lubrication mechanism comparable to synovial fluid (SF).

CHAPTER III

EXPERIMENTAL PROCEDURE

This chapter is an examination about the different materials used in this research. There are a variety of biomaterials employed for joint replacements. Metallic materials play a critical part as biomaterials to substitute the unhealthy or injured bone. Biomedical companies are primarily concerned to materials that are load bearing, resist corrosion , and compatible with the human body. Additionally, this research concentrates on enhancing biofluids for synthetic joints. There were four groups of materials analyzed and they were metals, ceramics, nanostructured materials, and lubricants. The lubricants were deionized water, bovine serum, synthetic fluid (SF), and simulated body fluid (SBF) all to be included in the materials section.

3.1 Materials

The metals utilized in this research were titanium (Ti) and titanium alloy Ti-6Al-4V.The ceramic used was alumina. The natural materials utilized were fullerene, hydroxylated fullerene, and crown ether. Additionally, there were lubricants, such as bovine serum, synthetic fluid, and simulated body fluid.

3.1.1 Titanium

The choice of material utilized for surgical implants is decided by the best execution. There are a number of good motives for utilizing titanium (Ti) as a prosthesis material. An illustration of this alloy is Ti-6A-4V [163]. Ti alloys subsist in trio crystal formation such as beta, alpha-beta, and alpha. [164, 165]. Additionally, titanium and its alloys have an elevated strength and lesser elastic modulus [166]. Ti has very superior

tissue compatibility and bears corrosion from contact with air and especially the human body [167].

Ti is appropriate for lasting joint replacement [167]. In addition, Pure Ti satisfies chemical homogeneity demands [167]. Several items, such as bone plates, screws, and instruments, are prepared from pure Ti [167]. Therefore, it can be assumed that using Ti as a prosthesis material can supply the utmost protection [167]. As indicated below in Table 9, Ti also has a low modulus of elasticity and high strength. In addition, Ti prostheses are chemically motionless and are free from corrosion [168].

Pure Ti was utilized as a counteracting material to examine the lubrication along with its wear behavior. The unpolluted titanium foil was from Sigma-Aldrich. Titanium foil sample was sliced in 2.54 cm wide x 2.54 cm height. Unpolluted titanium was putted in as the base for triobological experiments.

Titanium alloys, such as Ti–6Al–4V, are extensively used in many industrial fields. Titanium alloys are particularly employed as biomaterials because of elevated strong features to load ratio, lesser density, excellent fatigue features, outstanding corrosion opposition, and compatible with the body [40]. Titanium alloys as Ti-6A-4V are the most normally applied as metallic biomaterials [168]. The alloying of titanium has produced a superior outcome [169].They have been victorious due to their main characters of lesser density, being compatible to human body, elevated vigor, and corrosion opposition. The small density of Ti-6Al-4V is 4.4 g/cm3, which is near unpolluted titanium, which is 4.5 g/cm3. A further motive for its use is its being compatible with the body. Bio-compatibility has repeatedly been attributed for corrosion

results [170-172]. Ti-6Al-4V together makes it a superb material for joint prostheses because of its outstanding mechanical properties of titanium alloy. These mechanical properties are indicated in Table 8. A less elastic modulus reduces an elevated stress of the bone, consequential in less bone tissue shortage [173, 174]. Ti is a diverse element that can subsist in additional than one crystal structure [175].

As indicated in Table 9 [40,176], aluminum (Al) is weightier than vanadium (V) and is a little weightier than Ti. The density of Ti-6A-4V alloy is near pure titanium. The elastic modulus of Ti-6Al-4V is lesser than other metallic elements within the alloy. The advantage of this is it will cause less stress shielding [178].

Table 9: Mechanical Properties of Revised Titanium Alloys [40, 176].

Alloy	Tensile strength (MPa)	Modulus (GPa)
Ti (pure titanium)	785	105
Ti–6Al–4V	960–970	110

As indicated in Table 10 [175, 177], is the chemical composition of Ti and Ti–6Al–4V which determine influence the mechanical properties.

Table 10: Chemical Composition and Properties Ti and Ti-6Al-4V [175, 177].

Alloy	Wt%	Density g/cm^3	Modulus Pa
Ti-6Al-4V		4.43	105
Ti	Balance	4.51	110
Al	6.0	5.50-6.75	380
V	4.0	3.50-4.50	127
C	.10		
Fe	20		
H	.015		
N	.03		
O	.20		

Ti-6Al-4V alloy ball was obtained from TRD Specialties. The 6 mm diameter steel balls were utilized for the counter material in this tribological test. This tribological test was utilized to research the friction characteristics of alumina.

3.1.2 Alumina

Joint replacements have utilized alumina ceramics due to their elevated wear resistance. The usage has been limited due to problems related to functioning of these ceramics in the human body. It is known that the application of alumina mechanism in artificial joints leads to complications with unfastening femoral parts as a result of their

brittle performance. The main disadvantage is that ceramic is brittle; therefore, it would eventually be harmful to the human body.

Alumina was utilized as a substrate with water, simulated body fluid, and synthetic fluid as lubricants. The formula for alumina is Al_2O_3.

3.1.3 Fullerene

Since its discovery in 1985, the C_{60} has attracted great attention because of its exclusive structural and mechanical properties [179-181]. The novel groups of closed caged molecules were termed Buckminister Fuller, after the designer of this spherical structure [180]. There is a bonding likeness between graphite and the individual groups of C_{60} [182]. It was theoretically predicted that the C_{60} or C_{70} could be used as lubricants due to their spherical form and small cage diameter [182-185]. The C_{60} was reported to be able to elevate load power and to have small surface energy, elevated chemical steadiness, fragile intermolecular, and sturdy intramolecular bonding [179, 181, 186, 187]. The fullerene C_{60} could work as a ball bearing and for other tribological applications [188-190].

Fullerene C_{60} was used as a solid lubricant in deionized water. The structure of fullerene is a pure carbon molecule compiled of 60 atoms of carbon, as displayed in Figure 7. The solids were fullerene C_{60} from Sigma Aldrich

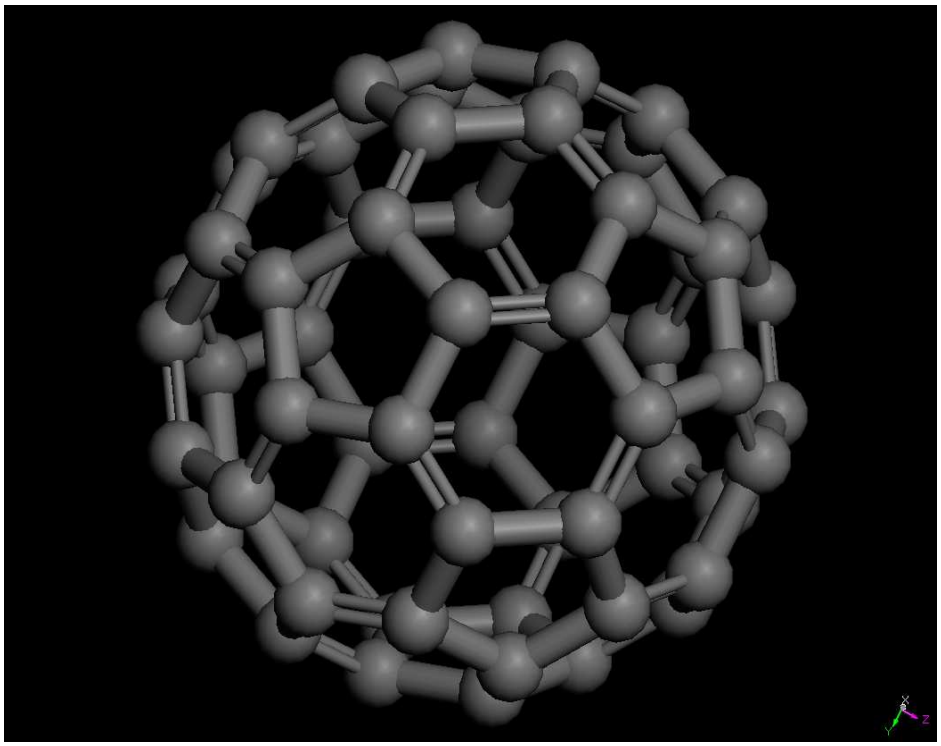

Fig. 7: Fullerene C_{60}. Simulated by Rohan Matthews.

.

An elevated level of water solubility occurs in the fullerene derivative when OH, COOH, or NH_2 fasten to every carbon in the fullerene cage [191]. They are competent contenders for several biomedical applications, which include cell defense, genetic photo split, enzyme restraint, diagnostic reflection, and others [191]. The reactive oxygen species, such as superoxide and hydroxyl (OH) radicals, can cause cell injury [192, 193]. In addition, the fullerene central part performs as a free radical sponge [192, 193]. The fullerene performs with a defensive effect in reactive oxygen species both outside and inside of an organism [192, 193]. The polydroxylated fullerene performs with a protection that produces the reactive oxygen species nerve cells' demise [192, 193].Specific fullerenols are polyhydroxylated fullerenes [C_{60} $(OH)_n$]. Fullerenols are

primarily regarded as antioxidants that decrease reactive oxygen species nerve cells [194, 195].

Fullerenol performance provides protection against stress in certain conditions of cell lines and certain conditions of rat lungs [196]. It reduces poisons against breast cancer cells of humans [197]. Fullerenol can cause cell death [196] and control the creation of human breast cancer cells [197]. It is stored in a specific protein, in spite of its outcome of not producing rapidly on rat fluid carrying blood vessels [198].
The pure fullerene investigation was delayed because of it insolubility in water [199]. However, pure C_{60} can be dissolved in water by mixing continually [200, 201]. The researchers described the malignant tumor of the liver cells in contrast with other water-soluble fullerenes [202]. In underivatized fullerene C_{60}, there was an analysis of largemouth bass whose brain was affected after two days of contact [203].

The FUH is displayed in Figure 8. $C_{60}(OH)_{24}$ was used as a solid lubricant in deionized water. The structure of fullerene is a pure carbon molecule compiled of 60 atoms of carbon with 24 hydroxyl groups. $C_{60}(OH)_{24}$ was used as a solid lubricant in bovine serum, and it was dissolved. The solids were fullerene $C_{60}(OH)_{24}$ from MR LTD. The DI water was used in order to avoid interactions of ion-nanoparticle interactions. The deionized water had no impurities and was a Newtonian fluid.

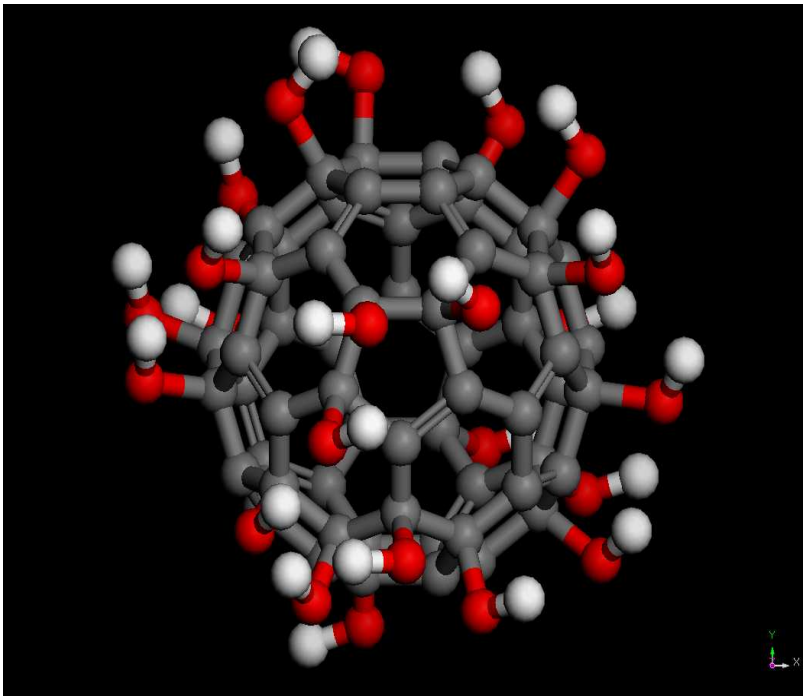

Fig. 8: Hydroxylated Fullerenes C_{60} $(OH)_{24}$. Simulated by Rohan Matthews.

3.1.4 Crown Ether

Since the discovery of crown ethers and their ion complexion abilities in 1967 by Pedersen [204], chemistry has emerged into rapidly increasing research topics [205]. The crown ethers have a unique flake-like structure that results from joining atoms in a 2D ring [206, 207]. They have led to the development of novel phase-transfer catalysts, artificial receptors, and ion channels. The fundamental recurring unit of any simple crown ether is ethylene, such as – $[CH_2CH_2O]$-, that replicates six times in 18-crown ether-6 [207]. The structure of crown ether is displayed in Figure 9. The general formula for 18-crown ether-6 is $[C_2H_4O]_6$ [208].

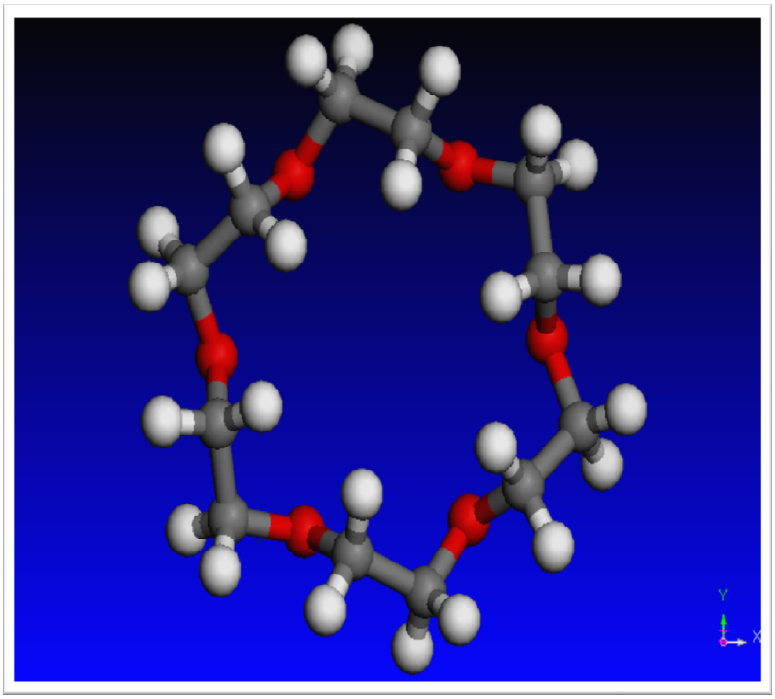

Fig. 9: 18-Crown Ether-6. Simulated by Rohan Matthews.

Crown ether has a high attraction for potassium, as indicated in Figure 10. In addition, crown ethers can be utilized to modify the features of inorganic mixture in organic liquid. When 18-crown-6 is present, potassium acetate is a more potent nucleophile in natural solvents than potassium acetate alone.

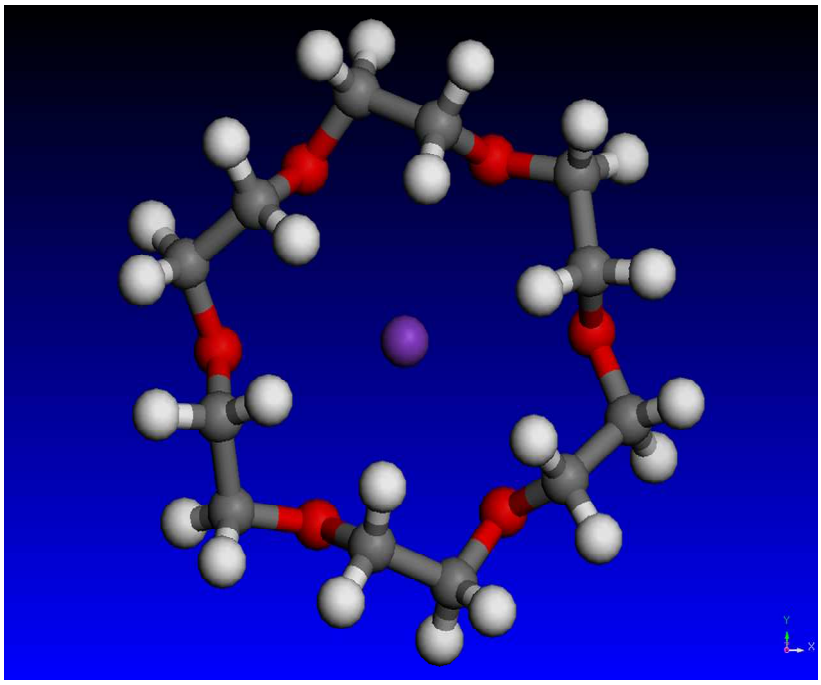

Fig. 10: 18-Crown Ether-6 Coordinated with Potassium Ion.
Simulated by Rohan Matthews.

In order to understand the mechanisms, we compare the fullerene C_{60} with a nanostructured 18-crown ether-6, as shown in Figure 9. DI water, crown ether/DI water, and fullerene/DI water were compared for lubrication performance. It was also discovered that crown ether has a tendency to form nanochains. This will be discussed in Chapter V.

3.1.5 Bovine Serum

Bovine serum is a synthetic fluid made from calf. Bovine serum of varying strength has been employed as an appropriate solution to imitate the pseudo-synovial fluid. Lubricant has recently been identified as one of the major factors in vitro wear

testing of joint implants [209, 210, 211, and 212]. It is accepted that bovine serum is a better lubricant than the DI water [213]. It remains to be established how it simulates the properties of human periprosthetic synovial fluid as a lubricant for polymer/CoCr bearing couples [213]. In this research, bovine serum was utilized as a lubricant between articulating surfaces. Bovine calf serum was obtained from HyClone, which was used as a lubricant between the articulating surfaces.

3.1.6 Simulated Body Fluid

To begin with, a mixture of simulated body fluid (SBF) was made from ingredients to be discussed later. This solution was beforehand made by Dr. Tadashi Kokubo [214]. SBF is a mixture similar to synovial fluid but with viscosity comparable to water. The technique of preparation of SBF is found in [215]. The synovial fluid contains 0.1 to 5 mg/ml of hyaluronic acid (HA [216]. The strength of 3 mg of HA was from Rexall, Inc. and was blended for each ml of simulated body fluid. The combination was then transferred to a sonicator for 10 minutes to liquefy the HA remains in the liquid. The synthetic fluid was stored in a refrigerator at 3 ^{o}C. This solution was utilized as a lubricant between the articulating surfaces prior to the tribological tests.

3.2 Rheological Measurements

Before measurement, the rheometer was auto zero, and this occurred after the machine had warmed for 10 minutes. The spindle number was entered as this was used to compute torque percentage, viscosity in centipoises, shear stress (dyne/cm^2), and shear rate (1/sec). These factors were input from one parameter to another. The spindle number was inserted putting in the speed of rotation, record viscosity, and torque

percentage. The liquid to be calculated was placed in a receptacle. Liquids flows that were not Newtonian liquids were examined through the compilation of viscosity figures over a series of shear rates. There were several points taken to get an average viscosity of all lubricants tested. The viscosity measurements were performed using the several test holders that were circular shaped containers of 1-5 ml, which were then cleaned with acetone or deionized water after each test, as indicated in the scheme in Figures 11 and 12. Measurements were repeated for three times with duration of 5 minutes each. The tests measured the viscosity, along with shear rate and shear stress.

The rheological properties of the SBF, water, synthetic fluids, water/FU, water/CE, and were measured utilizing the Brookfield DV-III Ultra Rheometer, as shown in Figure 11 and Figure 12.

The rheological properties of bovine serum, bovine serum/FUH, and water/FUH were measured utilizing the AG Magnetic Bearing Rheometer, as shown in the Figures 13 and in Figure 14. The parameters set for the rheometer were: temperature at 37^{o}C which is the body temperature, spindle set at 60 mm, the machine was calibrated for 30 seconds, and the spindle was cleaned with acetone after each test. The viscosity, shear rate, and shear stress, of the three lubricants were measured for rheological properties; and they were saved on the computer.

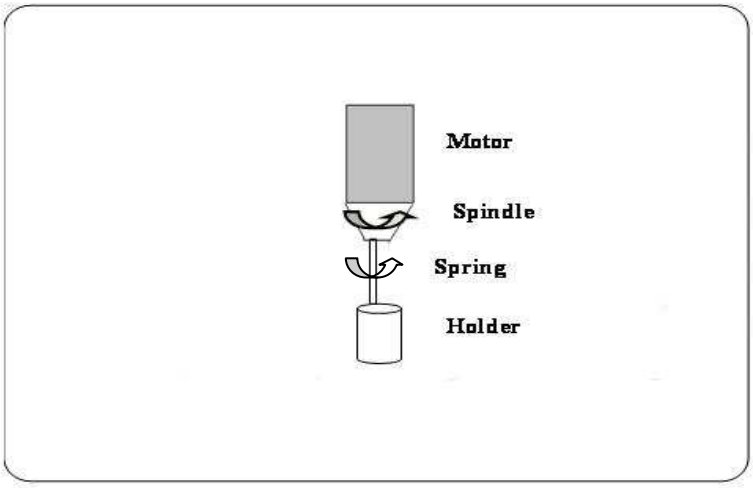

Fig. 11: Scheme of Brookfield Rheometer.

Fig. 12: Brookfield Ultra DV-III Rheometer [217].

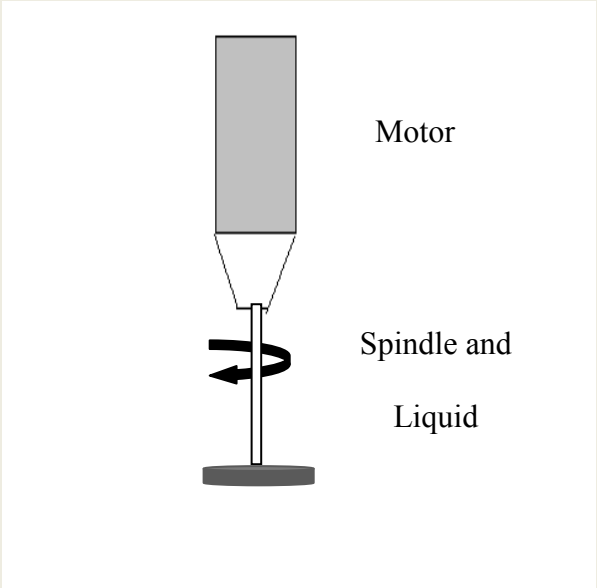

Fig.13: Scheme of Magnetic Bearing Rheometer.

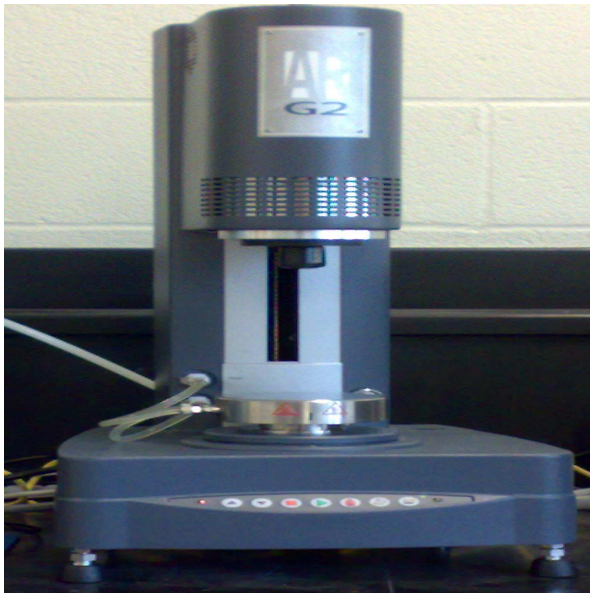

Fig. 14: AR-G2 Magnetic Bearing Rheometer.

3.3 Tribological Testing

Tribometers are unique instruments designed for precision friction force measurement. They can conduct both linear reciprocating and rotating modes. Tribological testing was done using a ball-on-disc tribometer, as shown in Figure 15, with the scheme displayed in Figure 16. The ball or pin material was fastened to the pin. The opposing material was fastened to a rotating attachment vertically below the pin. The pin was then fastened to a shaft that was joined to a transducer. When the attachment rotated, the frictional force of the articulating surfaces was communicated to a computer. A load was supported on top of the pin. After the computer determined the coefficient of friction, it then displayed a plan of the coefficient of friction against time. The parameters that could be regulated were reciprocating speeds, loads, time, along with the lubricant. This data was fed into the computer earlier before the test and remained constant throughout. These steps compared the friction coefficient of friction utilizing different lubricants.

In this experiment, the equipment used was a CSM tribometer. It utilized the ball-on-disk layout indicated in Figure 15 for tribological tests. The temperature was at room temperature of 27^{o}C. The motion was rotating-sliding for lubrication and reciprocating back and forth for wear tests. The loads, number of cycles, linear speed, and speeds were variable. The coefficient of friction against time was plotted using The TriboX software of the CSM Tribometer.

The lubrication and wear tests of water/FU, water/CE, and water were performed with parameters of different loads for lubrication and different speeds. For wear, the load and speed were constant.

For lubrication of bovine serum/FUH, water/FUH and bovine serum, the parameters were different loads and different speeds. For wear, using for these same lubricants, the parameters were constant load and constant speed.

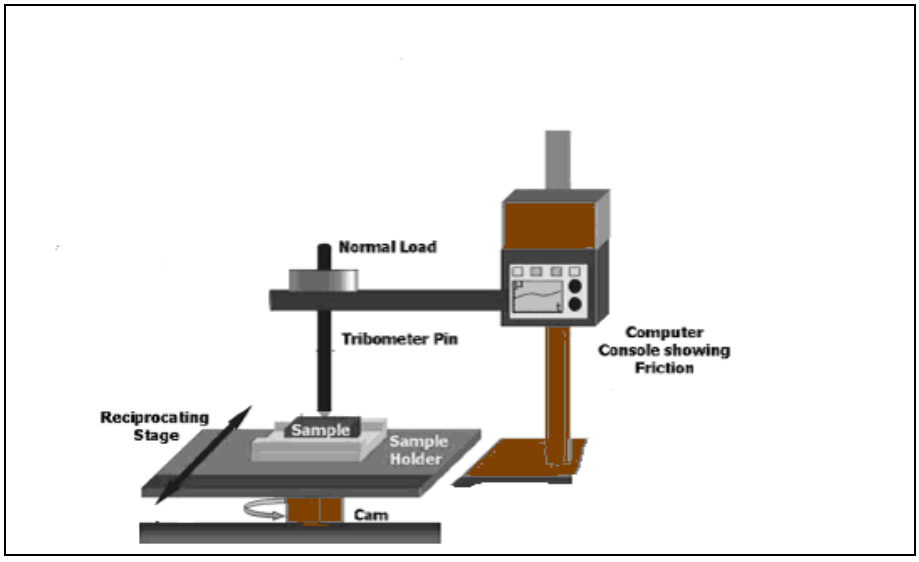

Fig. 15: CSM Tribometer Setup.

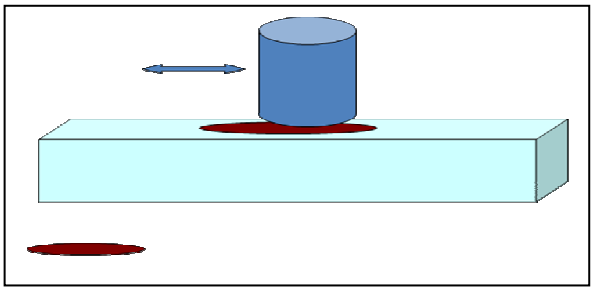

Fig. 16: Schematic of the Ball-on-Disk.

3.4 Characterization

There is a need for surface analysis both before and after conducting tribometer experiments to understand mechanisms of the tribological process. Various sophisticated surface characterization tools are available today to study the details of the surface, like morphology, surface parameters, and surface physical and chemical properties. The underlying general principle of most the majority of such instruments is the stimulus of a sample surface by means of a source signal and analysis of the resultant signal generated from the sample. Different methods mentioned below were utilized for surface characterization.

3.4.1 Surface Topography

The Profilometer is an instrument that maps a sample surface morphology. The contact mode was utilized in this experiment. The contact mode tip has a very receptive probe that slowly goes across a surface. The probe is generally made of a hard material like diamond and is somewhat rounded at the tip. The movement of this tip in the lateral and vertical directions is monitored by a controller that transmits the output signal to a computer. The screen displays a line profile of the traversed path. The sensitivity of this instrument is a few microns depending on the radius of the probe. The Profilometer also measures the roughness and waviness parameters of the surface using one of the standard methods available.

The non-contact Profilometer is an optical that uses white light. This technique has shown to be much better than laser techniques in measuring roughness. The optical Profilometer uses a non-contact method that supplies the same data as a stylus contact

Profilometer. There are there main advantages to an optical Profilometer. The first advantage is speed because there is no contact. The second advantage is reliability because they do not touch the surface and surface cannot be damaged. The third advantage is spot size, which ranges from a few micrometers to submicrometers.

The measurement principles consist of measuring the roughness of a surface part and then trace the surface at a constant rate. The pickup acquires the surface roughness by the sharp stylus. The roughness causes displacement of pickup, which results in a change of inductive value of induction coils that generate analogue signal, which is in proportion to surface roughness at the output end of a phase sensitive rectifier. Qualitest TR200 Surface Profilometer, shown in Figure 17, is employed to take the wear profile generated due to tribochemical actions. It helps in measuring the wear depth and also the surface after the formation of a tribofilm. Details of the operations of the scheme of Profilometer are displayed in Figure 18.

Fig. 17: Qualitest 200 Profilometer.

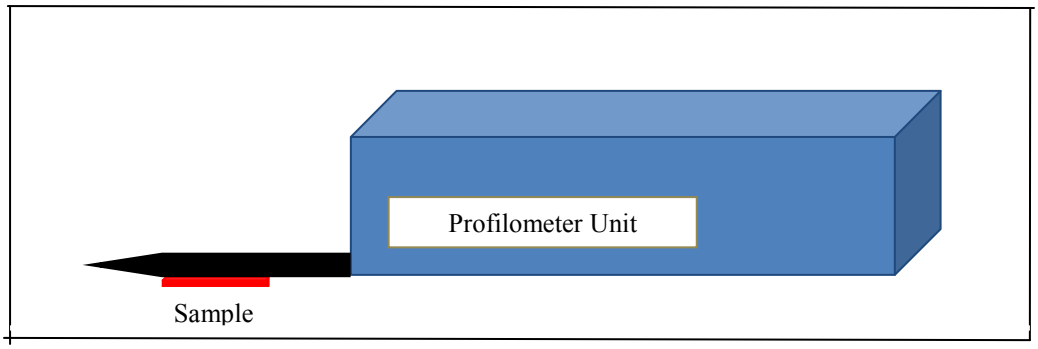

Fig. 18: Scheme of Profilometer.

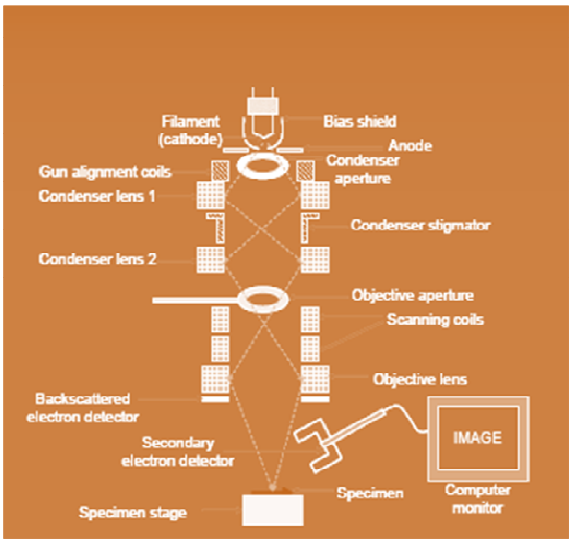

Fig. 19: Scheme of Scanning Electron Microscope [218].

Some of the elements utilized in SEM are comparable to the elements in TEM [219. They are the electron source, which consists of the gun, condenser lenses, objective lenses, and scanning coils [219. The ray goes through the objective lens before attaining the specimen [220]. The scanning electron microscope (SEM) is a type of

electron microscope where a fine beam of electrons are scanned across the surface of the sample [220].The scanning electron microscope scheme is shown in Figure 19. Descriptions of the sample can be conquered by distinguishing either backscattered electrons mirrored from the exterior or by indentifying the resultant electrons that breakout from the atoms of the specimen [220]. The principle of SEM is very simple and can be easily understood [220]. The scanning coils produce the pattern that creates the image on the computer screen.

The JEOL 6400 scanning electron microscope as displayed in Figure 20 was used to obtain images of the surfaces. Images were captured from secondary electrons. The working voltage was 15 kV, and the working distance varied.

Fig. 20: JEOL JSM 6400 Scanning Electron Microscope
Microscopy and Imaging Center, Texas A&M University [219].

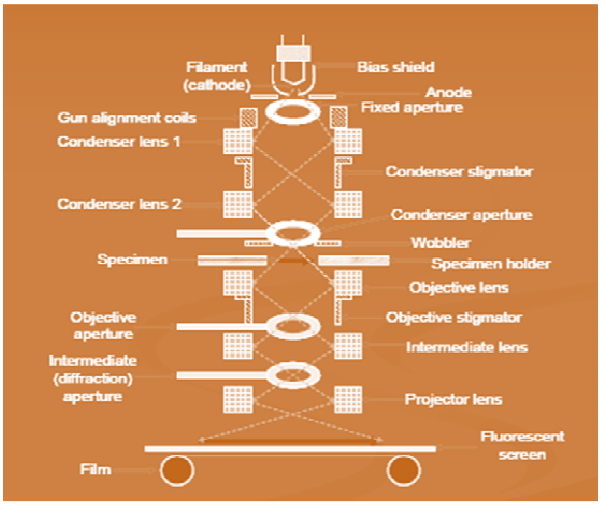

Fig. 21: Scheme of Transmission Electron Microscope [218].

3.4.2 TEM Studies of Nanoparticles

In a transmission electron microscope (TEM), a ray of electrons are transported through a thin specimen. The first potential outcome is the electrons are conveyed through the specimen without any contact. The second possible outcome is the electrons are swerved but have no force. The third potential outcome is the electrons' energy is lost and is turned aside [219]. Electrons with the smallest action with the sample have elevated energy when accumulated by the detector. The image yield from the detector consequently displays these components of the specimen as lighter [219]. There are potential outcomes for these electrons [220]. As a result, the last image is a black and white picture of the component of the specimen during which the ray of electrons passes throughout.

The imagery and patterns of wear fragments were acquired from the friction tests were attained with a Transmission Electron Microscope (TEM, JEOL JEM 2010) as shown in Figures 21 and 22. Samples for testing were collected in the form of wear particles from the specimen wear tracks after the tribo-tests. The wear particles were collected and dissolved in acetone for 10 minutes using a sonicator for microscopy characterization. The particles before and after the wear tests were examined using the TEM instrument having an accelerating voltage of 200 keV. A drop of dilute acetone solution containing the particles was placed over a carbon coated Cu grid, dried in air, and imaged with a TEM instrument.

Fig. 22: JEOL JEM-2010 Transmission Electron Microscope
Microscopy and Imaging Center, Texas A&M University [218].

CHAPTER IV

LUBRICATION PROPERTIES

As discussed in Chapter I, many biofluids are in the body. Of significant interest are synovial fluids that lubricate the joints. Many times the natural joints deteriorate due to diseases known as arthritis, or some other disease of the bone. There is a promising solution arthroplasty of the joints that is available to treat the deteriorated natural joints. The main problem is the wear of these artificial joints and diseased natural joints, which is due to inadequate lubrication. It is needed to optimize the lubrication of joints. In this chapter, we review the existing data of lubrication properties of biofluids. The present research focuses on a synthetic fluid made from hyaluroncic acid and simulated body fluid. Direct comparisons between viscosities, shear rate, and shear stress are carried out. The biofluids compared are from dogs, horses, humans, simulated body fluids (SBF), and synthetic fluids. Most recently, the focus is on nanostructured biofluids such as bovine, bovine/FUH, and water/FUH. The shear rate and viscosity of these biofluids are compared. This enables us to develop a baseline for new understanding of lubrication properties of biofluids for artificial joints.

4.1 Viscosity

Viscosity causes the resistance to flow. The SBF is a Newtonian fluid like water. In Chapter III, the SBF was described in detail. Dr. Tadashi Kokub initially arranged the SBF [213]. Tris (hydroxymethyl) aminomethane and HCl buffers were utilized to lessen the pH to 7.25 [213]. In Chapter III, ionic concentrations of SBF can be found in [214]. The strength of HA in synovial fluid was described as 0.1 to 5 mg/ml [215].The studies

of animal synovial fluid have established significant likeness among species. Yet, some notable differences do subsist. The amount of synovial fluid (SF) differs from joint to joint. In their study, five dogs were removed for testing [221]. SF from three dogs with chronic condition and two dogs with an acute condition were aspirate. The chronic joint symptoms displayed a slightly higher viscosity compared to those with acute symptoms [221]. As indicated in Figure 23, the viscosities of acute joints were lower, and this was due to the local inflammation and swelling of the joints [221]. In the chronic joints of the dogs, the viscosity decreased due to destruction of hyaluronic acid minor to osteoarthritis [221]. . In an early study by Conrad et al., normal joints exhibited considerably elevated synovial fluid viscosity compared to either chronic or acutely injured dogs, as illustrated in Figure 23 [221].The normal viscosity was highest, as expected.

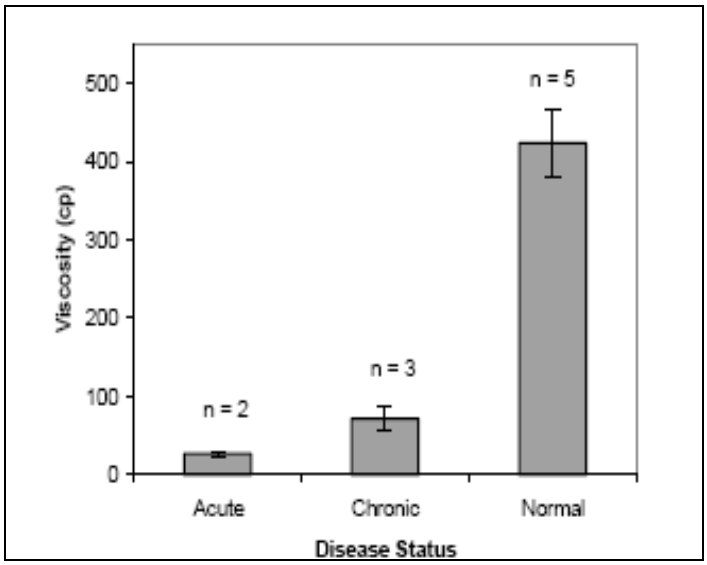

Fig. 23: Viscosity of Dogs with Different Level of Disease Status [221].

It is obvious that the horse viscosity behaves like the SF. With the horse SF, as the viscosity decreased as the shear rate increased which is indicative of shear thinning. Lumsden evaluated the apparent viscosity of normal SF of mid-carpal,

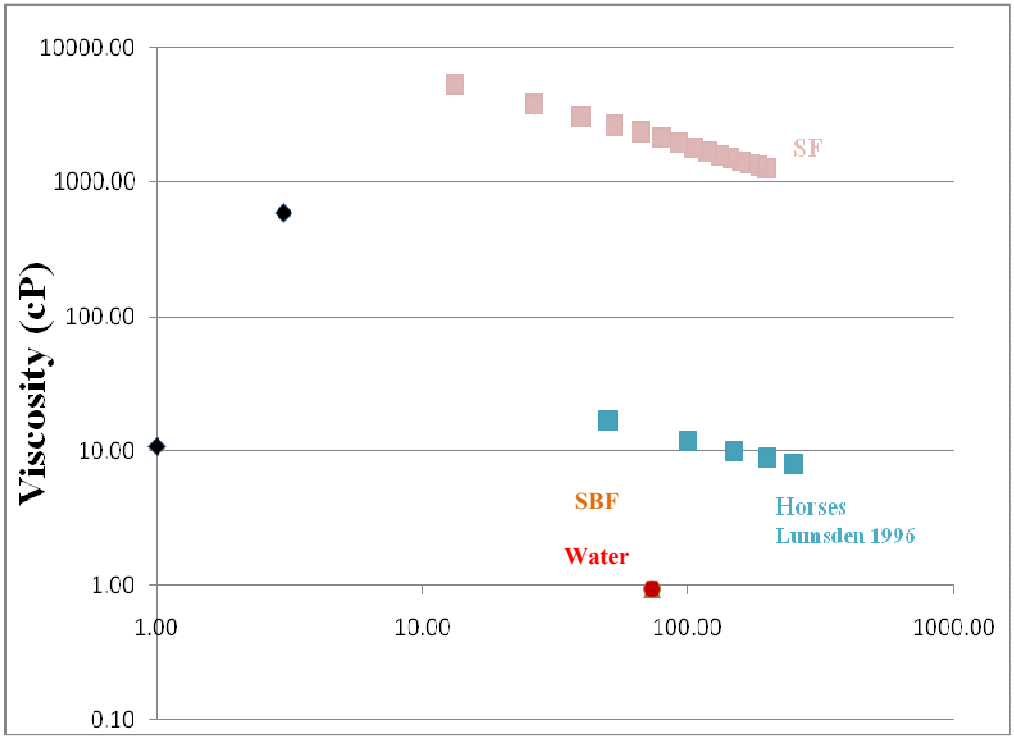

Fig. 24: Comparison of Viscosity vs. Shear Rate of Synthetic and Live Fluids .

Lumsden evaluated the apparent viscosity of normal SF of mid-carpal, tibiotarsal, and distal interphalangeal joints of horses [222]. The apparent viscosity was assessed with variable shear rates. It resulted in the assessment at a known shear rate and temperature [222]. The viscosity of SF was measured in poises in proportion to shear stress to rate of shear, which is a non-Newtonian fluid [222]. The plan included viscosity evaluation in a range of shear rates that was utilized to differentiate the apparent

viscosity of four SFs' from three joints [222]. In this study, there were 60 clinically normal horses [222]. In Figure 24, the SF is similar to that of horses and that of human as indicated in Figure 25. The synovial data from SF was gathered from samples that were acquired over a shear rate of 10 to 250/s. In addition, it was collected at apparent viscosities that were calculated at 50, 100, 150, 200 and 2501/s [222]. The result of shear rate on apparent viscosity was resolved utilizing a two-way Analysis of Variance (ANOVA) [222]. The outcomes for the SF from all the joints denoted shear-thinning behavior. In this figure, apparently, with an increase in shear rate there is a decrease in the viscosity.

Lumsden did similar comparisons [222]. The horse viscosity behaved like the SF that is similar to the human's. As the shear rate of the horse SF increased, the viscosity decreased, which indicate shear thinning as indicated in Figure 25. The data for horse viscosity was from reference [222]. The horse viscosity is similar to normal human viscosity, as indicated in Table 11

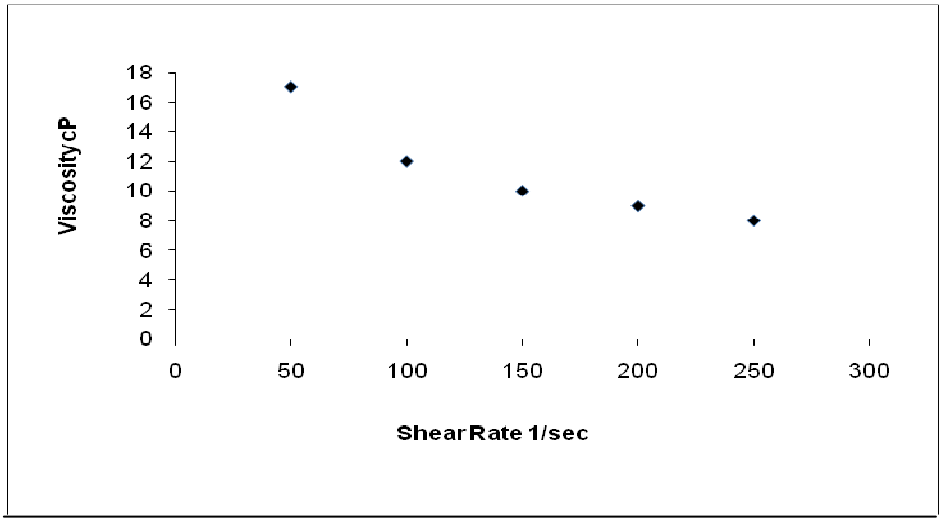

Fig. 25: Apparent Viscosity for Ten Clinically Normal Horses [222].

Table 11: Relative Viscosity of Synovial Fluid [223].

Species	Joint	Diagnosis	Volume, ml Avg.	Viscosity Avg.
Horse	Carpal	Normal	5	929
Horse	Carpal	Normal	6	16
Human	Knee	Osteoarthritis	32	106
Human	Knee	Rheumatoid Arthritis	29	18
Human	Knee	Chronic traumatic	32	20

In their earlier study, Levine et al. [224] provided results of viscosity of synovial joints from normal and pathological types of human arthritis. Comparative viscosity was established in 65 normal fluids from animals and 287 pathological effusions [224]. The main values, and also the widest range of viscosity, were obtained from the normal fluids of the carpals joints of cattle [224]. Fluid form the carpal joints of horses displayed a narrow range and a much lower average relative viscosity [224]. Several factors must be considered to explain the discrepancy between the cattle and horses [224].

As stated earlier, the viscosity of synovial fluid of horses is similar to the synthetic fluid. In examining the synthetic fluid, the shear rate increased as the viscosity decreased behaving like shear thinning fluid. As stated earlier, this was due to the hyaluronic acid content. The hyaluronic acid is a polymer whose formula is Hyaluronan (HA). The HA is a high-molecular-weight material that is present in plentiful amounts in synovial fluid. It is the main source of viscosity of synovial fluid. In Chapter I, HA is in a greater amount than any of the other molecules.

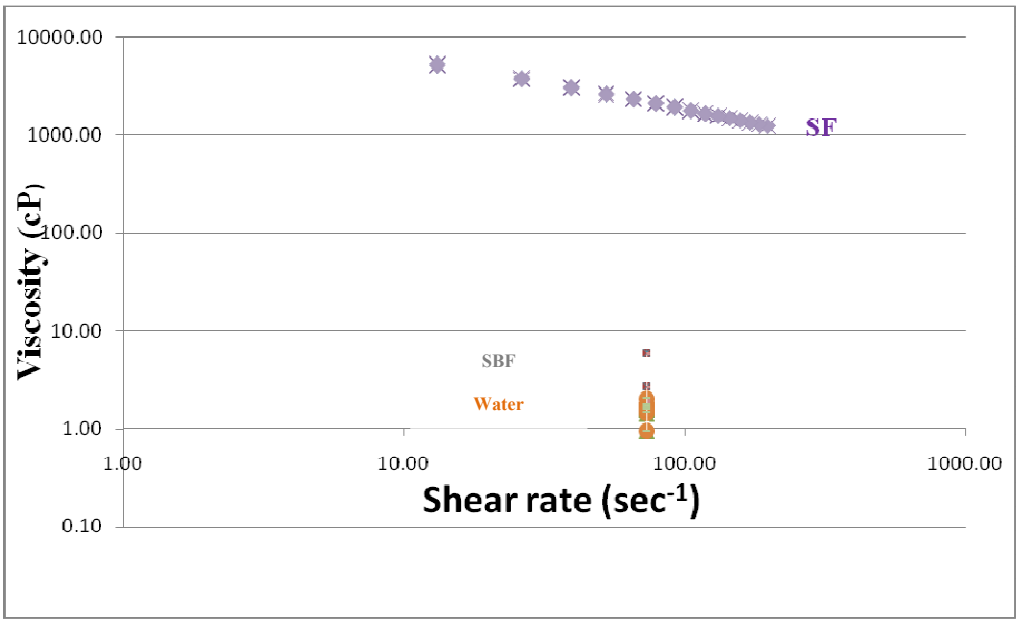

Fig. 26: Comparison of Viscosity vs. Shear Rate of Synthetic Fluids.

The synthetic fluid consists of SBF and HA. The description is described in detail in Chapter III. As stated earlier, the hyaluronic acid is the source of viscosity of synthetic fluid. The make-up of the synthetic fluid included 3 mg of HA acquired from Rexall, Inc. It was mixed per ml of SBF. The mixture was then exposed to sound waves for about 10 minutes for dissolving the hyaluronic acid fragments. The synthetic fluid was stored in a cooled storage place at 34 ^{o}F. The viscosity of the mixture was applied as a coating between the rubbing surfaces before the tribological tests. The synthetic fluid shear rate behaved like the horse and opposite to the SBF and water, as indicated in Figure 26. As indicated earlier, the HA causes the viscosity in the SF. In addition, the synthetic fluid, synovial fluid in horses and dogs, along with humans, has hyaluronic acid content. As seen in Figure 27, with the synthetic fluid, as the shear stress increased,

the viscosity decreased that indicate linearly relationship. With this synthetic fluid, although the viscosity behaved like a human's, but the friction was unstable and was not suitable for the human joint.

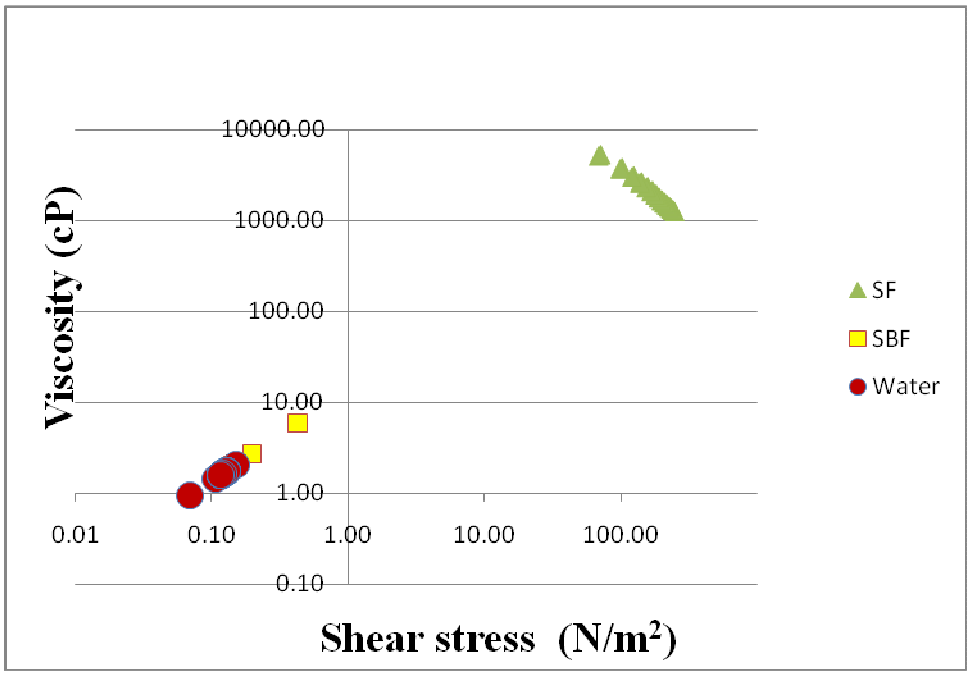

Fig. 27: Comparision of Viscosity vs. Shear Stress of Synthetic Fluids.

These lubricants exhibit three kinds of interactions between apparent viscosity and shear rate. The types are Newtonian, thixotropic and dilatants as indicated in Figure 28. The shear stress and shear rate relationship is a straight line called Newtonian fluid. The correlation between viscosity and shear rate is displayed as stable in Figure 28. Thixotropic and dilatants are non-Newtonian fluids. Dilatant liquids are when the viscosity increases with increases in shear rate. Thixotropic fluids undergo decrease in viscosity with time. Conventional ones have viscosity that is independent of shear rate.

Therefore, surface separations as a function of relative viscosity may be determined fairly easy, taking the lubricant properties as constant. Under these conditions, the type of lubrication may stay constant over a wide range of velocities.

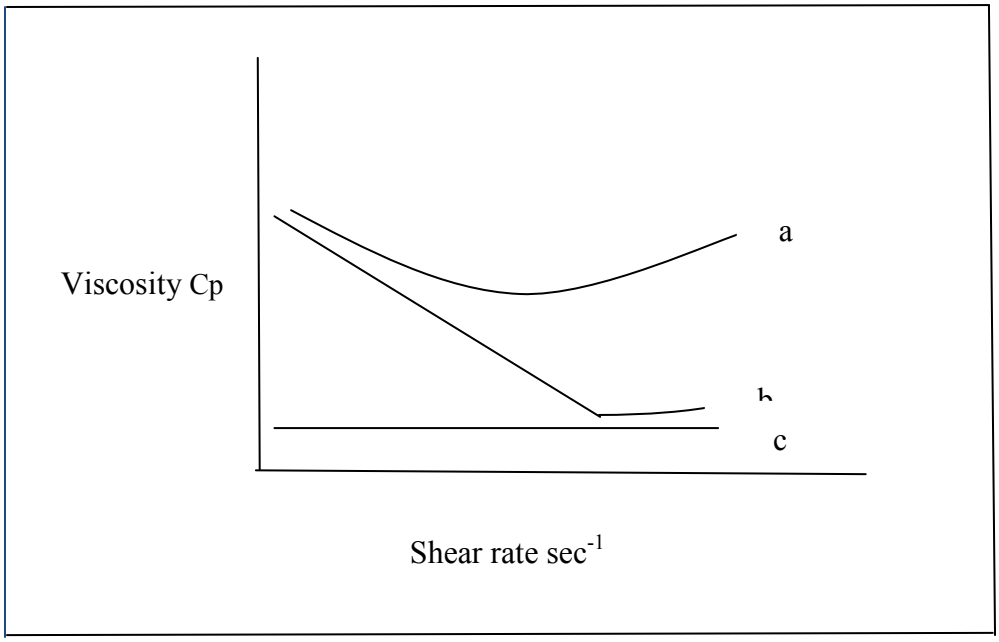

Fig. 28: Lubricant Types: a) Dilatant, b) Thixotropic, c) Newtonian (not scale) [38].

Some lubricants are thixotropic; they turn around and become less viscous as shear rate increases [38]. The thixotropic or dilatants lubricants can make a alteration in lubrication modes due to the relative speed of the surface [38]. For example, a pair of materials with thixotropic lubricants can exhibit full film lubrication [38]. They can display at midway loads and speeds along with boundary lubrication at high loads and speeds. Synovial fluid is made of a hyaluronic acid and it is an exceedingly thixotropic lubricant. Injury may reduce the movement of the fluid causing a less viscous but still thixotropic

lubricant [38]. Nevertheless, in the incidence of rheumatoid arthritis, the synovial fluid both water down thins and will lose its thixotropic property [38]. This contribution permits closer approach to deterioration of joint surfaces and can generate wear. The synthetic fluid and the horse viscosity act approximately like dilatants fluids, as seen in Figure 24. The water and the simulated body fluid in Figure 24 behave like Newtonian fluids.

As for human fluid, it is difficult to get the results of viscosity of a normal synovial fluid. This is clarification that my synthetic fluid is not suitable, because as indicated in [222], the viscosity decreases with increased shear rate for the normal, osteoarthritis, and rheumatoid arthritis. Osteoarthritis and rheumatoid fluid viscosity is less, and the fluid is nearly Newtonian [223].However, in the study by Wright and Dowson, the synovial fluid is a non-Newtonian in that its viscosity decreases with increased shear rate [225, 226]. The viscosity-shear rate relationships of normal synovial fluid demonstrate that it is non-Newtonian. They are similar to the viscosity displayed in horse fluid. The only significant difference is with the normal start at a higher viscosity. The viscosity for normal synovial fluid is higher for humans, and for two samples, osteoarthritis (OA) along with rheumatoid arthritis (RA), it has the same tendency but at a lower viscosity as indicated in Figure 29.

The viscosity of nanostructured biofluids displays a relationship that illustrates that as the shear rate increased, the viscosity is decreased. As the viscosity increases, it thickens, and it resists flow. As the viscosity decreases, like with water, it does not resist flow, and the shear rate increases. As stated earlier, viscosity causes a resistance to flow.

As the temperature of the lubricant is amplified, the viscosity will lessen. For instance, in the chart above, the viscosities were measured at two different temperatures for the nanostructured biofluids. One set was measured at room temperature of 25^{o}C as displayed in Figure 30, and the other set was measured at the human body temperature of 37^{o}C was indicated in Figure 31. For all of the mixtures, as the temperature increased, the viscosity decreased. This kind of association was displayed for normal, OA, and RA, indicated in an earlier study. In Figure 30, the viscosity-shear rate relationship of bovines behaves like the osteoarthritis and rheumatoid fluid, and it is Newtonian. The viscosity-shear rate relationships of normal SF show that it is non-Newtonian with the highest viscosity.

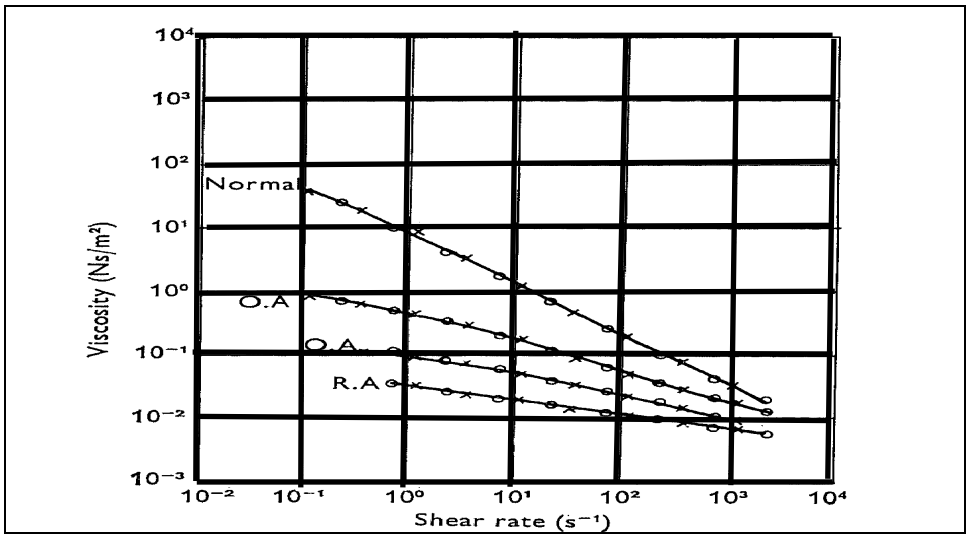

Fig. 29: Viscosity of Shear Rate Relationships [223].

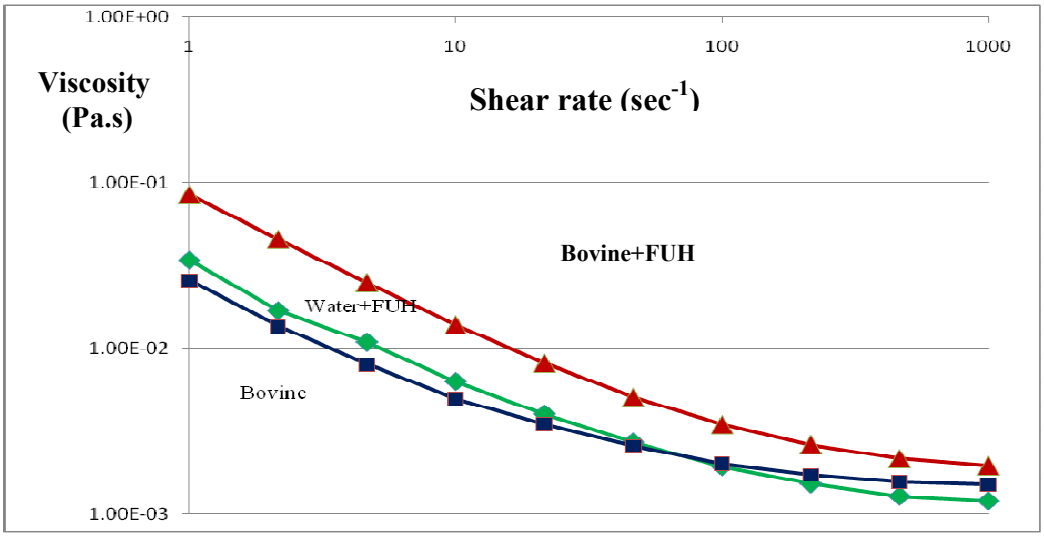

Fig. 30: Comparison of Shear Rate vs. Viscosity of Nanostructured Biofluids at 25°C.

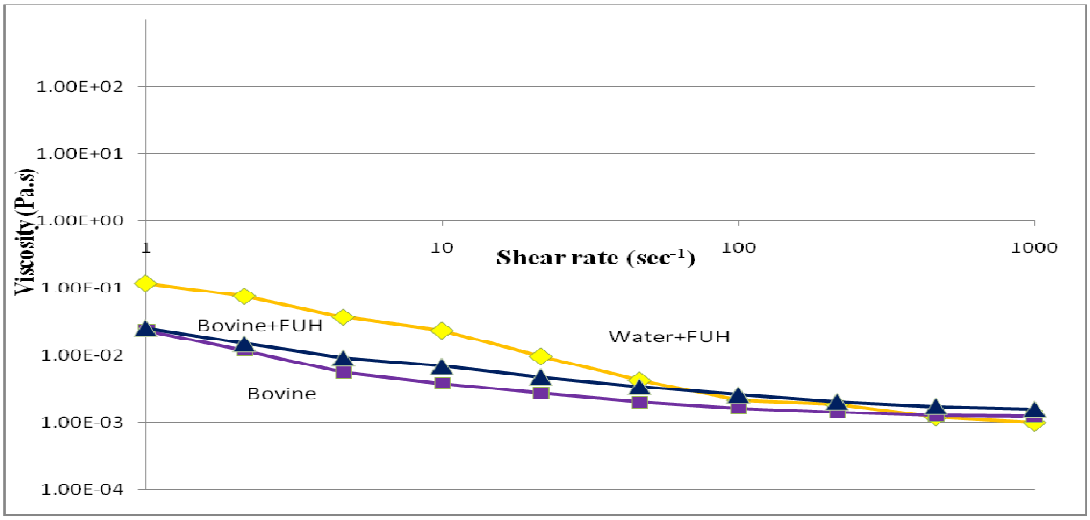

Fig. 31: Comparison of Shear Rate vs. Viscosity of Nanostructured Biofluids at 37°C.

4.2 Viscosity Relation to Friction

Friction is defined by Black [38] as opposing the movement and rubbing one material over the other [38]. Friction coefficient is a dimensional number that is the ratio of friction force to normal force. It is obvious from Table 12 that artificial material couples do not come near the friction coefficient of natural joints. There is nothing that can be done as long as body fluids are relied upon for lubrication [38]. Still, it is determined that coefficient of friction is greater when surfaces first begin to move than when the surfaces are in motion [38]. See Table 12, which denotes condition of coefficient of friction and μ_s as the sliding coefficient of friction. The basic information above confirms tribological testing that follows.

Table 12: Revised Initial and Sliding Coefficient of Friction [38].

Materials grouping	Lubricant	μs
Cartilage/cartilage hip	Synovial fluid	0.002
Cartilage/cartilage hip	Ringers	0.01-0.005
Co-Cr/Co-Cr hip prosthesis[236]	None	0.55
	Veronate buffer	0.22
	Serum	0.13
	Synovial fluid	0.12
	Albumin	0.11
Co-Cr/UHMWPE [236] Weightman et al. 1972 [236]	Serum	0.08

In Chapter III, the tribological testing was done on several lubricants to measure the coefficient of friction. Water and SBF are both Newtonian fluids. The synthetic fluid behaved like a puesdoplastic fluid. The synthetic fluid was made from SBF and HA. The tribological tests were conducted for two hours. The plots were friction coefficient against time. The water was sliding against alumina in the presence of water. Alumina is a hard ceramic with hard elements established at room temperature [227]. It suggests many potentials of generating mechanisms with useful patterns of features comprising tribological functions. The components of ceramic provide well in a variety of media [227]. Major diversities exist in the tribological performance of various ceramics in water [227-232]. Furthermore, the introduction of water at the edge made the creation of hydroxides, along with other composite to water, media probable [229]. Water causes the unconfined wear debris to be cleaned off constantly. This occurred on the sliding exterior, and an ideal adhesion was supplied [229]. The performance of these material arrangements were considered deprived in sliding contacts. The creation of loose wear debris may cause instability in moving mechanical groups [229].

Researchers have recommended that aluminium hydroxides are formed on the mating surfaces [233]. This is due to the high interfacial temperatures produced during the application of pressure in the midst of water [233]. The formation of ferrous transfer The layers of oxide ceramic discs is formed on ferrous transport. This is observed in unlubricated contacts with similar materials [234, 235]. Prior to materials being investigated in the body, the HA coating must be spread over the metal [236].

In the water sliding test, the coefficient of friction was constant at 0.4. The overall friction coefficient during this test was constant. The plot indicated that the water was stable. During the absence of SBF, at the interface, the conditions approached those of a dry test, causing an increase of friction coefficient. It is significant that the synthetic fluid contains HA along with SBF. HA is the source of the viscosity of any fluid. This can account for the high viscosity; however, it does not exhibit good frictional properties. In the synthetic fluid sliding test, the friction coefficient began at 0.38 and decreased to 0.15. This may be due to insufficient concentration of the solution. In these experiments, it was discovered that the synthetic fluid combined of SBF and HA, the viscosity behaved most favorable viscosity/shear rate like a real fluid. With the nanostructured biofluids,

CHAPTER V

NANOSTRUCTURED BIOFLUIDS

Fundamental understanding of nanostructured biofluids possesses significant scientific and technological importance. In this research, we proposed to use well-defined molecular or nanostuctures to modify biofluids in order to develop new insights from lubrication theory and application. This chapter focuses on the basic lubrication properties of such biofluids.

5.1 Background

In natural joints, the synovial fluid is stored in the synovium membrane. The functions of synovial fluids are to provide lubrication to the joint and nutrients to the cartilage. Disease, such as arthritis, and/or injury may require artificial joint replacement. During total joint replacement (TJR), the synovial membrane is altered, and the synovial fluid (SF) is lost [237]. The lost SF is replaced by a periprosthetic SF. This fluid is a natural lubricant generated in vivo after an artificial joint surgery [238-240]. To date, there are few reports on the periprosthetic fluid. Problems remain in the TJR, namely lack of lubrication and resulting wear leading to the malfunction of the acetabular cup of the prosthesis [241]. In attempts to improve engineering lubrication outside of TJR, nanostructured additives have been used. Fluids with nanostructured additives are called nanofluids. It was reported that nanofluids had good dispersion and adhesion onto a solid surface, providing satisfying structural, optical, and thermal properties [242-244].

In the current research, we propose to study effects of shapes of certain molecules on lubrication. Fullerene C_{60}, was used as additives for this study. The property-tribological

performance relationships of fullerene nanostructured biofluids were studied. In order to understand the mechanisms, we compared the fullerene C_{60} with a nanostructured 18-crown ether-6, a 2-D ring structure. Detailed information of fluid missing was discussed in Chapter I. The experimental procedures for fluid properties were discussed in Chapter III.

5.2 Rheological Properties

The viscosity vs. shear rate of H_2O, CE, and FU is plotted, and results are shown in Figure 32. The FUH viscosity vs., shear rate is higher than FU. All four fluids show non-Newtonian behavior. It is interesting that the addition of CE increased the viscosity, while that of FU significantly reduced and the addition of FUH increased viscosity higher than FU. The water and CE fluids both show thinning, while the FU is mostly consistent in the range of shear rate. The viscosity and shear stress represent the intermolecular interactions between fluid molecules and additives. Comparing the C in FU in a previous (Figure 7), and O in CE previous (Figure 9), the CE is more electronegative and is prone to attract water molecules. The strong Van der Waals attraction between CE and H_2O results in high fluid shear and viscosity. It is known that water molecules interact with each other through hydrogen bonds. In order to understand the behavior further, we studied the frictional behavior of fluids.

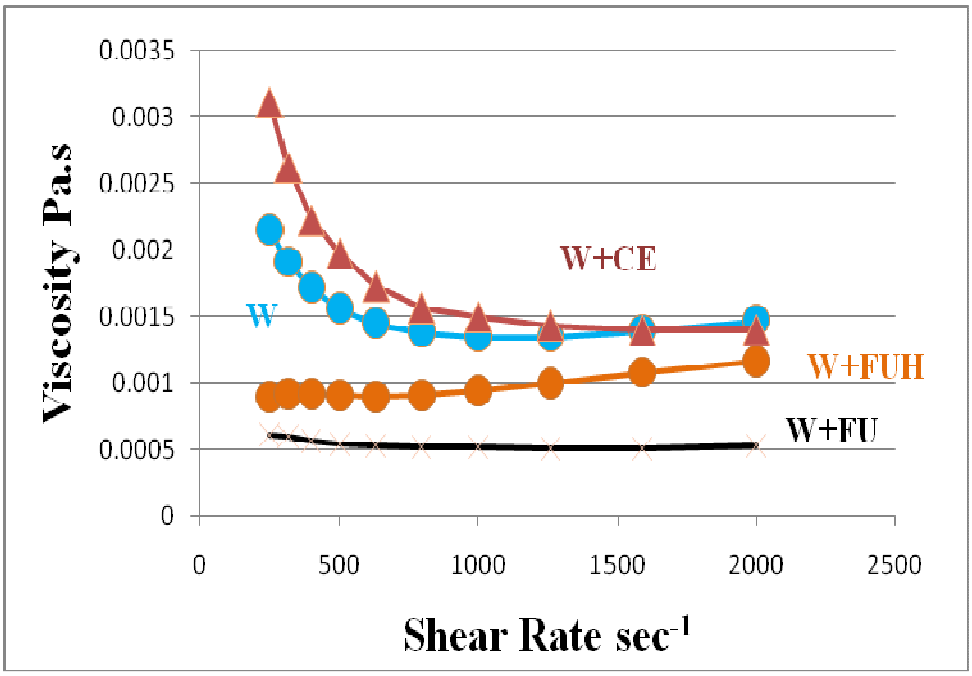

Fig. 32: Rheological Results of Three Fluids.

5.3 Nanoparticle-Modified Fluid Friction

Our viscosity results have shown that all fluids have shown non-Newtonian behavior. The addition of fullerene, in particular, resulted in significant reduction in viscosity and shear rate. This means that the FU-containing fluids require less force (or energy) to shear the fluid (Figure 32). This will subsequently reduce friction (this will be discussed in the next section). It is well known that the fluid shear stress can be expressed as,

$$\tau = \eta \frac{v}{z} \qquad (3)$$

where τ is the tangential (friction) stress between the fluid layers, η is the friction coefficient of a fluid, i.e., the viscosity, v is the linear speed, and z is the thickness of the fluid. The fluid shear can also be formulated as,

$$\tau = \eta \frac{\partial v}{\partial z} \qquad (4)$$

where the $\partial v/\partial z$ is the shear rate (velocity/thickness). It is noted that this equation is similar to that of shear strength of materials, $\tau=G(\Delta x/\Delta z)$. Here, the τ is the horizontal force required to deform the surface, G is the shear measure of stiffness, and $\Delta x/\Delta z$ is the ratio of disarticulation in x- and z- directions. In a liquid, it is seen that the elastic energy applied to a lubricant is a function of the rate of energy. Similar to the elastic modulus of a solid, G; the elastic modulus of the fluid, η represents the "stiffness" of a fluid. It is related to the "adhering strength" of fluid molecules. Our viscosity results showed that the addition of FU has significantly reduced the viscosity value at any shear rate. This could be due to the "adhering strength" of fluid and water molecules, as mentioned. The FU has weaker bonding strength with H_2O than CE, although both have Van der Waals attraction. The reduced attraction between FU and H_2O enhances the fluidability, thus, results in low viscosity and shear.

5.4 Effect of Nanostructures on Fluid Lubrication

What are fundamental lubrication mechanisms using nanostructured particles for our study? The "Stribeck" curve was obtained from three fluids tested, as shown in Figure 33. The friction coefficient was plotted against a group of parameters (viscosity·speed/load). In Figure 33, H_2O and CE had similar frictional behavior, i.e., friction increased quickly at the high load and low speed range and stayed high at 0.6. While for FU, the friction remained low and increased to a stable value of 0.2. The three curves did not appear as having typical lubrication regimes, i.e., boundary, elasto-hydrodynamic, and hydrodynamic lubrication. Particularly for H_2O, the lubrication layer was never formed. This means that all three fluids have the boundary lubrication-like behavior. The initial friction might be due to the interaction between water and surfaces.

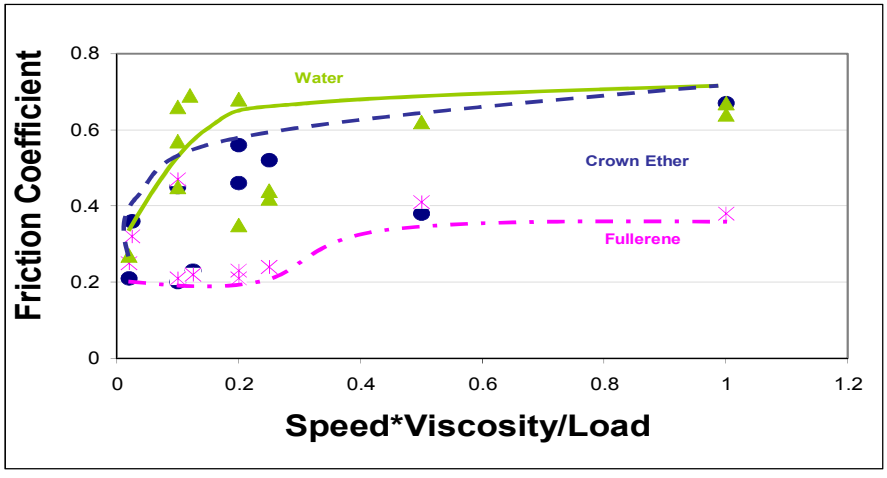

Fig. 33: Friction Coefficient against the Grouping.

In order to find out the interactions between fluid and additives, we conducted a TEM analysis of CE and FU before and after wear tests, as shown in Figure 34. Here 34a (top left) is a CE particle in water before wear tests; 34b (top right) is the aggregated particles of CE after wear tests. These two figures indicate that the CE aggregated together due to friction. This phenomenon is believed to not be beneficial for a low friction. Figure 34c (bottom left) is the TEM image of a FU particle before wear tests and 34d after. Clearly, it is seen that the FU particles were physically broken down and became small particles. In addition, it is clear that the energy required to roll a ball is significantly less than rolling a flake, as illustrated in Figure 35.

As mentioned earlier, the attractions between C (in FU) and water molecules is relatively weak compared with O-H_2O (in CE) interactions. The spheres, having weak attraction with water molecules, are expected to roll under shear stress. The low friction (Figure 33) and the low viscosity (Figure 32) of FU support this statement. The lubrication property of fullerene C_{60} has been reported. When it was added to oil, the friction between steel and copper was reduced [246].

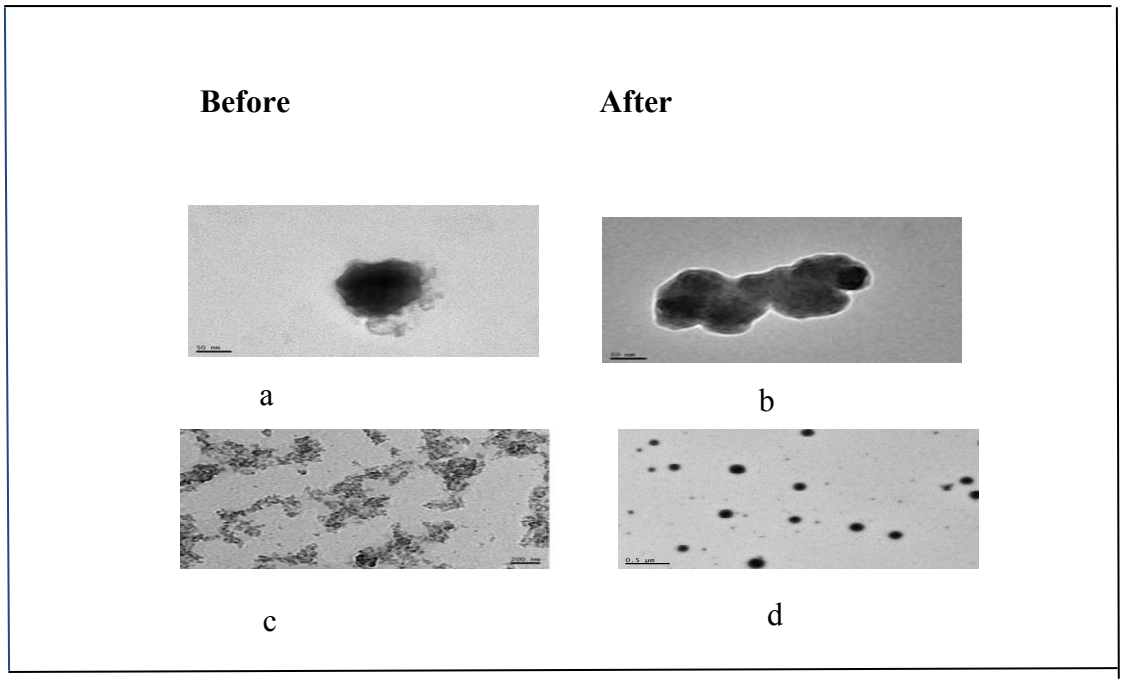

Fig. 34: TEM Analyses of Nanostructures.
a: CE Particle in Water before Wear Tests; b: CE Aggregated Particles after Wear Tests; c: Image of FU Particle in Water before Wear Tests; d: Image of FU Particle after Wear Tests.

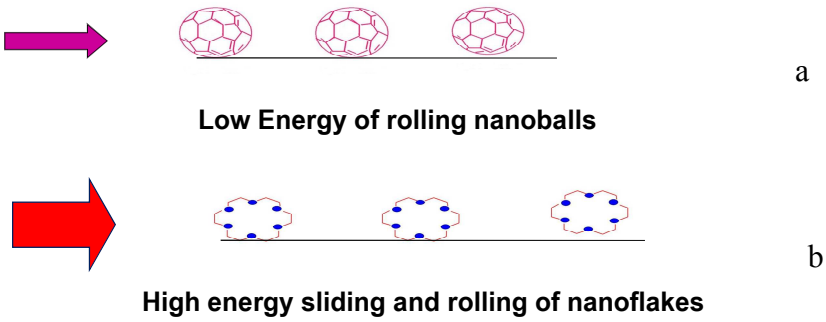

Fig. 35: Schematic Comparison of Nanofriction.
a: Nanoball; b: Nanoflake.

5.5 Tribological Tests

The friction and wear were tested against time using the pin-on-disk apparatus. Figure 36 and 37 shows the wear results. Figure 36 shows the depth of the wear track using a profilometer. The top version is the standard deviation. Here, the FU provided the least wear and water and CE had similar and higher wear depth. The surface quality was obtained using an AFM scanning inside the wear track. Results indicated that the surface obtained using FU was actually polished (Figure 37). The wear mechanisms were further analyzed using the SEM, and results are shown in Figure 38. Figure 38a is the as-received sample surface with random scratches; 38b is the wear track obtained from CE, and it seems to have a thick layer detached with scattered debris. Figure 38c is from FU and it has uniform grooves. Some debris lie on the wear track surface. The FU appears to generate the least wear, and the surface is the smoothest (Figure 38b).

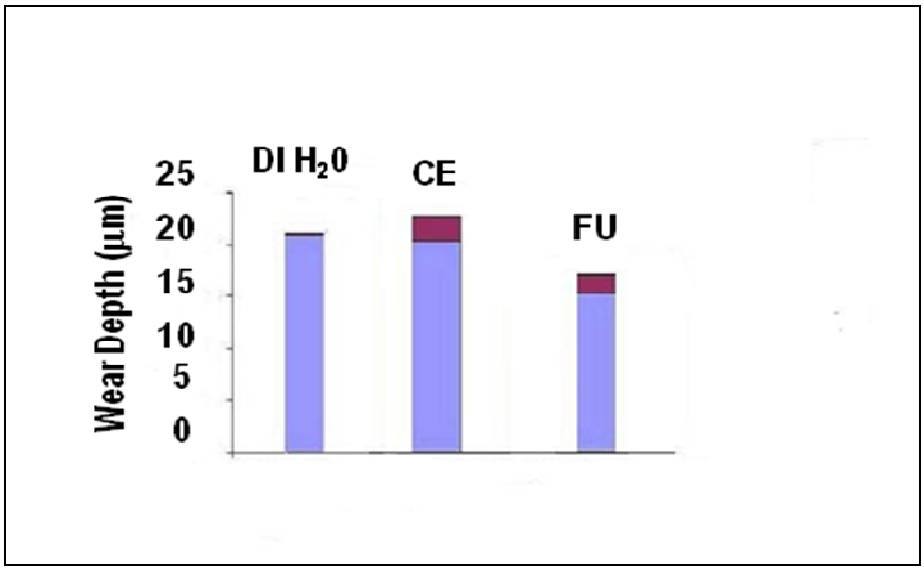

Fig. 36: Wear Depth of Nanostructured Biofluids.

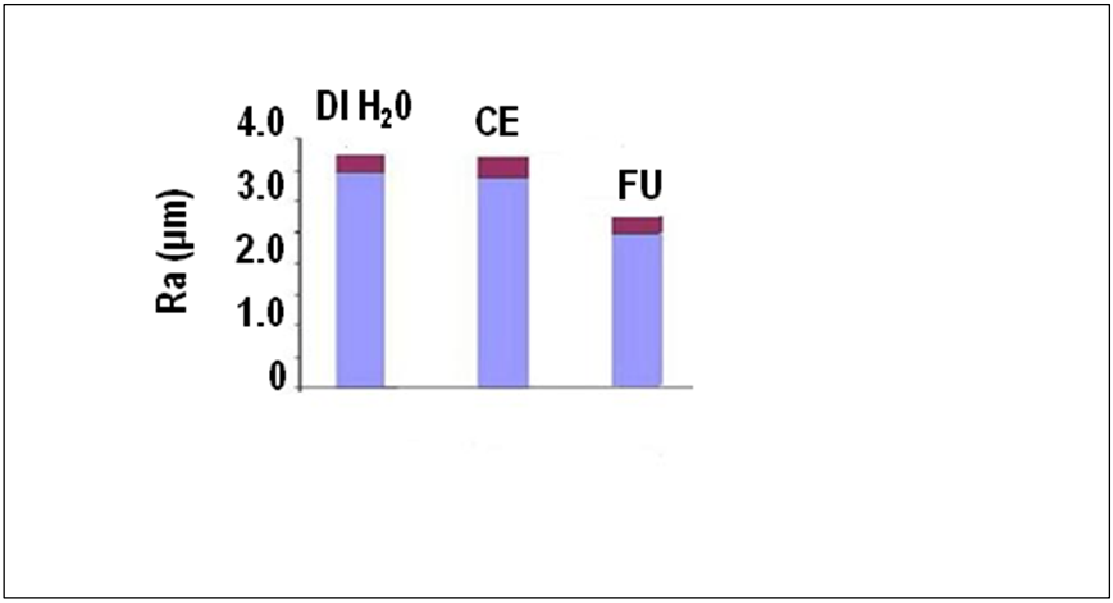

Fig. 37: Surface Roughness of Nanostructured Biofluids.

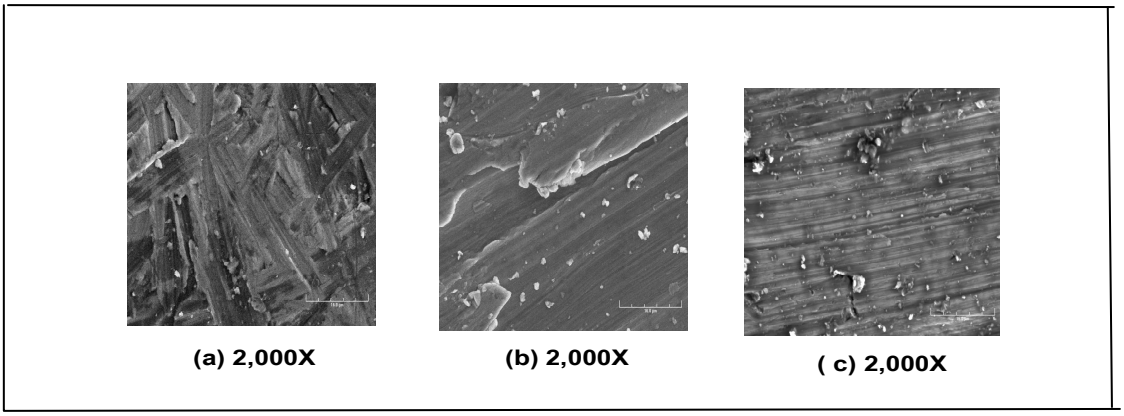

Fig. 38: SEM Micrographs.
a: Original Titanium Surface for Reference;
b: Crown Ether Wear Particles from Sliding in DI Water;
c: Fullerene Wears Particles from Sliding in DI Water.

5.6 Friction and Wear Behavior

As shown in the friction results (Figure 33), under sliding, the FU provided the lowest friction when compared to two other fluid samples. These experiments were obtained at a condition where the boundary lubrication condition was expected. The fact of FU providing least resistance to sliding is in correlation with the viscosity and shear data. Our results showed the evidence of FU reducing fluid resistance and friction.

What are effects of fluids on wear? As results show in Figure 36, the FU promoted the least wear. It is noticed that both CE and FU are dry powders in dry conditions. When added into DI water, they did not act as abrasives. The low viscosity and low wear in the FU case means that the FU is a lubricant. In the case of water and CE, the relatively high wear might be related to mechanical and/or tribochemical interactions, as mentioned earlier.

The friction obtained in the present work is similar to previously reported results. The coefficient of friction of ultra high molecular weight polyethylene (UHMWPE) against refined metals and ceramics during simulator experiments were between 0.03 and 0.1 [244-248]. The friction coefficient provided by FU is comparable to the literature value [249]. The coefficient of friction obtained for FUH is higher than FU.

This research opens a new avenue to design biofluids using nanostructured additives. Our next steps are to focus on the interactions between tissue and nanostructured additives and to develop an applicable biofluid. We will continue to test other rubbing pairs. In the human body, the cartilage has a thick and viscoelastic protein layer that maintains a certain amount of liquid for lubrication [250]. Current artificial

joints are not properly lubricated and their curved surfaces can not be lubricated using conventional concepts of lubricants. Although the bio-compatibility and stability of the FU have not been studied, the methodology proposed here is promising for artificial joint lubrication.

5.7 Interfacial Reaction Induced Nanostructures

In consideration of biocompatibility, the hydroxylated fullerene (FUH) was tested as a comparison to traditional FU. For bovine and bovine/FUH, the frictional curves were similar and do not indicate any significant information. For the FUH, the frictional curve in Figure 39 was similar to FU in Figure 33. Clearly, it is seen that the FUH and FU particles were physically broken down and became small spheres. The main advantage is that FUH is not toxic to human cells, but the disadvantage is it has a higher coefficient of friction.

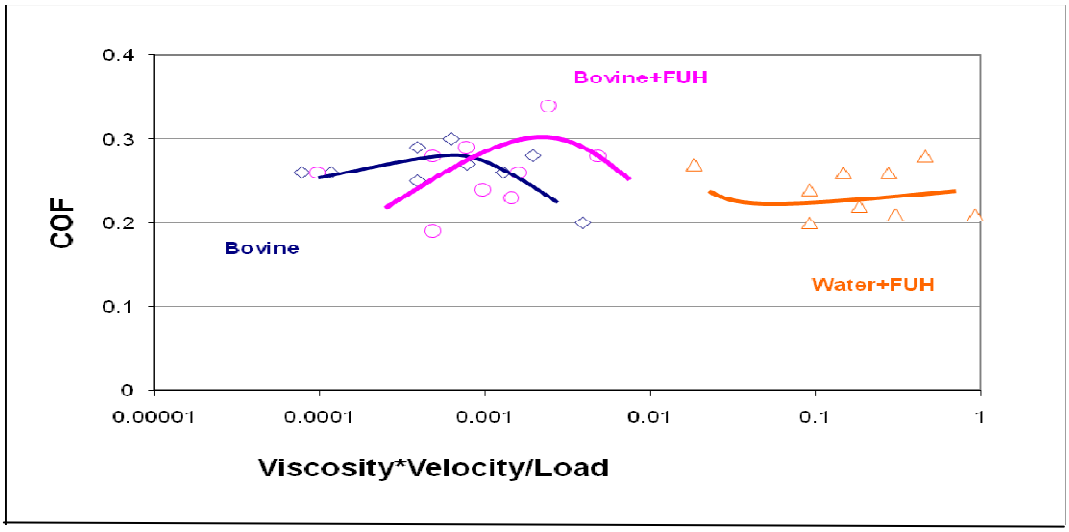

Fig. 39: Nanoparticles Lubrication Mechanisms.

In addition, in order to find out the interactions between fluid and additives, a TEM analysis was conducted of bovine/FUH and water/FUH before and after tests, as shown in Figure 40. Here 40a is a FUH particle in bovine before wear tests; 40b is the cluster particles of FUH after wear tests. These two figures indicate that the FUH reacted with each other through friction. In Figure 40c, the TEM image is of FUH particle in water before wear tests, and 40d is after the test.

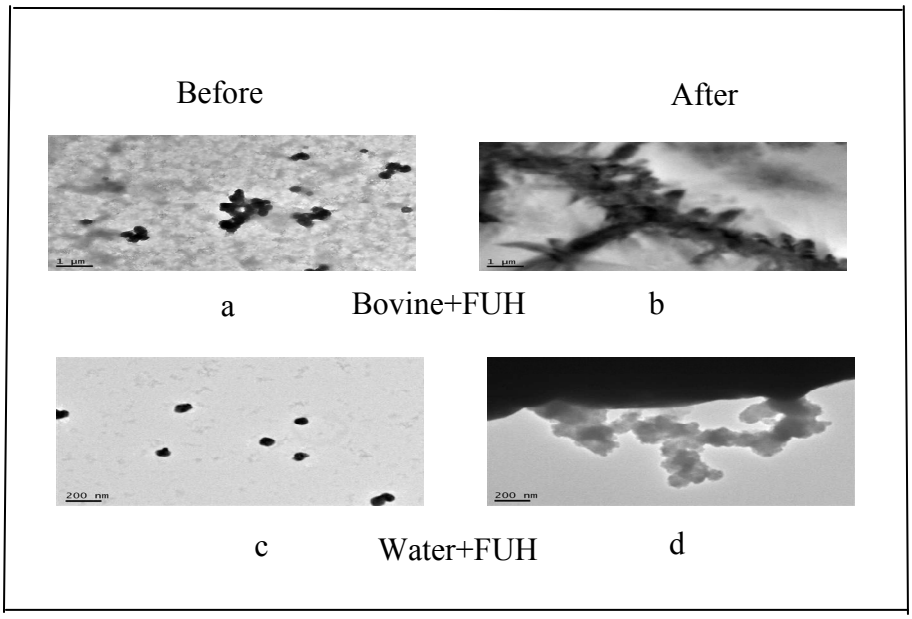

Fig. 40: TEM Analysis.
a: FUH Particle in Bovine before Wear Tests; b: FUH Aggregated Particles after Wear Tests; c: Image of FUH Particle in Water before Wear Tests; d: Image of FUH Particle after Wear Tests.

Using nanostructured bio-compatible additives to lubricate artificial joints is a promising method and will be further studied. Current artificial joints are not properly

lubricated, and their curved surfaces cannot be lubricated using a conventional concept of lubricants. Although the bio-compatibility was not studied here, the methodology proposed here is promising for artificial joint lubrication.

5.8 Tribochemical Reactions of Crown Ether

Pederson discovered the CE in the 1960s and received the Nobel Prize for his discovery. The ring-like CE has a cavity size of 2.6 – 3.2 Å. Under strain, the CE can be strengthened and distorted with a particle broken ring [251]. In the present work, we processed the CE under sliding force. TEM samples were obtained before and after tests, as shown in Figure 41. In the figure, the size of our crown ether is significantly larger than that reported in literature [252]. Figure 41a is the overall TEM image of crown ether particles. Figure 41b is a large particle of crown ether of a ring structure. The cavity size is about 50 nm, and the ring thickness is around 55 nm. Based on the size, these are mainly aggregated molecules. The center cavity might be due to the surface tension of formed aggregates. Figure 41c is the image of a particle of 60 nm. There are some whiskers attached to the particle. This might be due to the distorted molecules of crown ether.

CEs' after testing are studied using the same TEM, as shown in Figure 42. Interestingly, all molecules after testing have become chain-like. Figure 42a is the typical 2-D structure of the tested particle. There are nodules in dark color and chains in light. Typically, the size of the nodules is around 50 nm, and the average length of the chains is around 105 nm (Figure 42b). That means that the distance of each nodule is around 1-5 nm. Similar nanochain structure has been reported in crystalline Silicon (Si)

[253-255], Silicon Oxide (SiO), [256], Gold, (Au) [257, 258], Nickel (Ni) [259], and Cobalt (Co) [260] with much longer chain length (>10nm) through more complicated processes. The nanochain structures and processes reported have not been reported.

In order to understand the nature of those nanochains, we analyzed samples using an EDS and UV. Figure 43 shows EDS results of samples before (43a) and after (43b) tests. Before experiments, there are peaks of copper (Cu), oxygen (O), and carbon (C) This was confirmed by the EDS attached to TEM, as shown in Figure 43 .There appeared to be no specific peak due to effects of water. .The Cu was from the mash holder for TEM sample. C and O are from the CE. While in 46b, new peaks of Ti were found. This means that the nanochain nods are trapped Ti. This indicates that the Ti ions were formed due to rubbing and then wrapped by the distorted crown ether. The UV-Vis spectroscopy data, as shown in Figure 44, displays two curves representing samples before and after experiments. The curve of solid line (or above) indicates the absorption spectra of the sample before test. It had no specific absorption peak, but a narrow band ranged from 208-215 nm for the ring structure of the crown ether moiety. After the sliding tests, the band changed to a broad absorption band found in the range 210-270 nm, as indicated by the fragmented line in Figure 44. This means that the circle arrangement of crown ether was destroyed due to friction. The incorporation of Ti ions in the CE molecule successively increased the molecular weight of the compound.

The present work reveals that when using CE as a template, nanochains can be formed due to rubbing. The CE is known to bond positively charged ions. At the interior

of the cavity, the oxygen atoms react, which traps the ion metallic particles. Under sliding, the CE breaks down and is reattached to form chains.

Rubbing two surfaces to produce nanochains is an extremely simple and cost-effective method to synthesis nanostructures [261]. The friction force involved during rubbing not only provides tangential force to remove titanium ions, but also promotes formation of rods, leading to nanostructures.

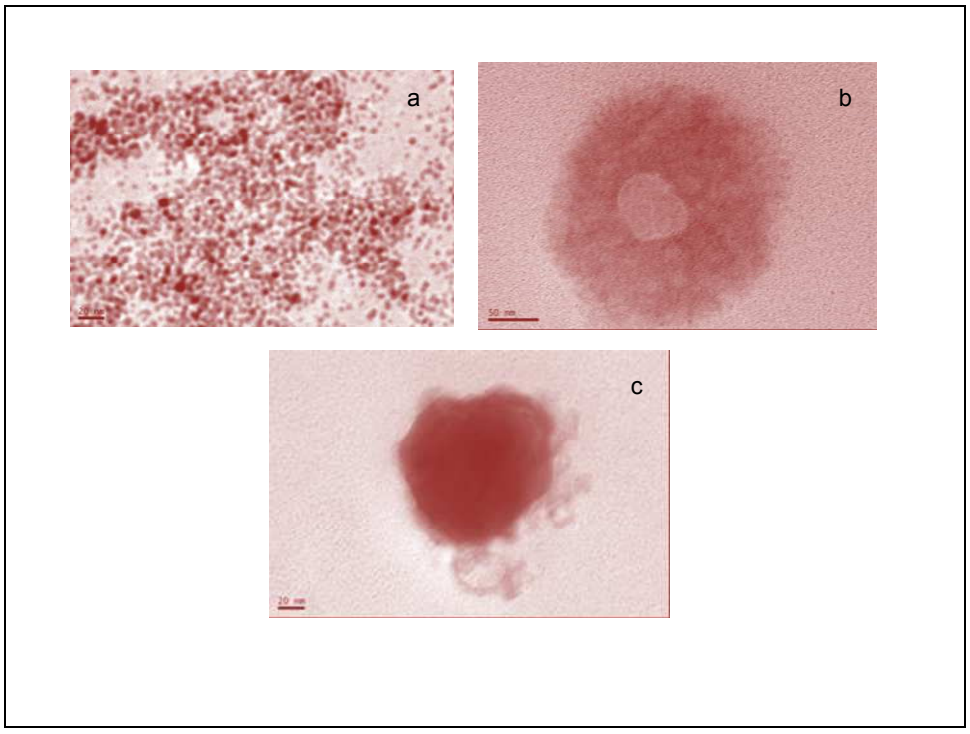

Fig. 41: TEM Images of Samples before Tests. (a) Overall Sample Particles; (b) One Ring-like Structure; and (c) One Particle of Aggregates of Damaged Crown [261].

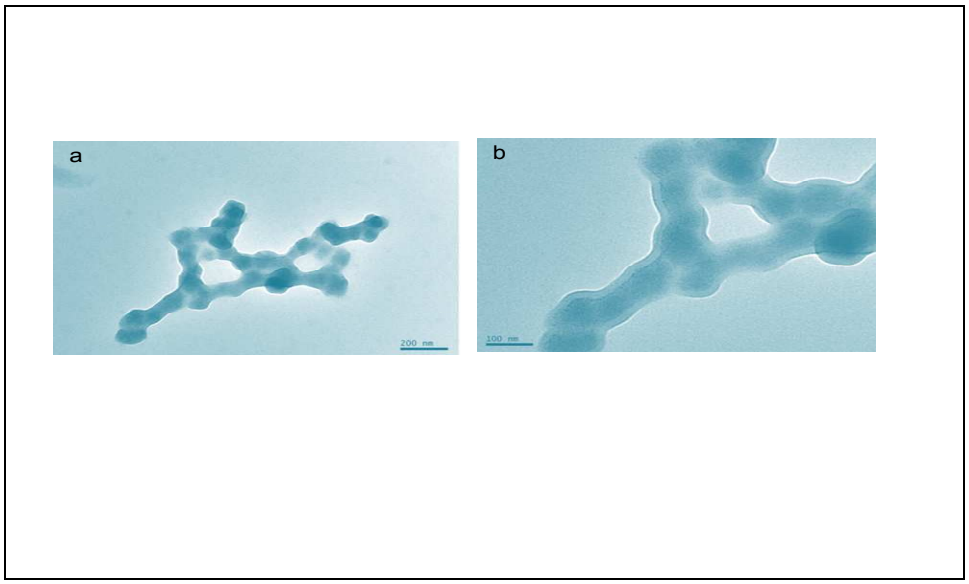

Fig. 42: TEM Image of Samples after Test Showing Nanochain Structure [261].

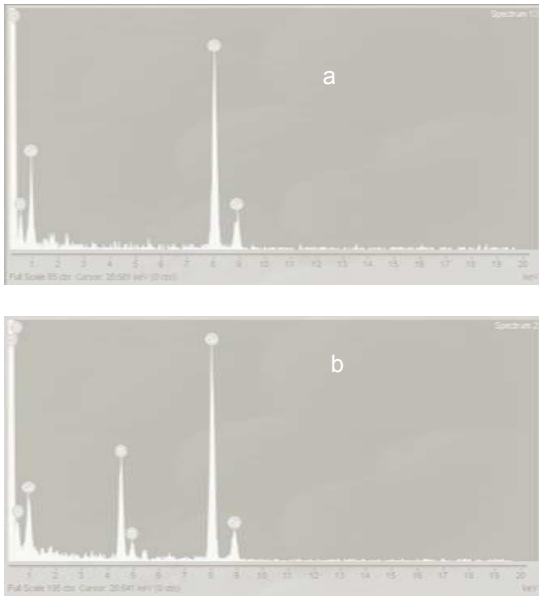

Fig 43: EDS Analysis before (a) and after (b) Tests [261].

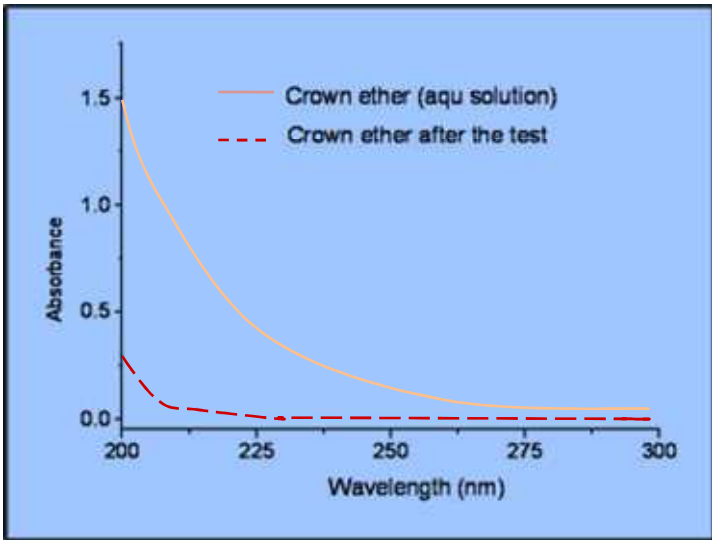

Fig. 44: UV-VIS-NIR Spectra Comparing Samples before (top curve) and after (bottom curve) Tests [261].

This chapter discussed effects of nanostructures on biofluid lubrication and resulting nanochain structures. The FU promotes lubrication with rolling mechanisms while crown ether requires more energy to do so. The friction force was found to introduce nanochain structures with crown ether. Ionic Ti was trapped by the distorted CE, forming unique nanostructures.

CHAPTER VI

SUMMARY AND CONCLUSIONS

Tribological examination of nanostructured biofluids was performed for the relevance of joints prosthesis lubrication. Outcomes illustrated that the summation of fullerene nanoballs to deionized water could decrease the coefficient of friction coefficient during the boundary lubrication mode. The friction and wear were mutually amplified, when adding crown ether flakes to deionized water. Microscopic inspection displayed proof of configuration of nanoballs. The lesser heating lead to the benefit of applying nanoballs, while lesser energy associated with lesser wear. The opposing idea is that flakes call for elevated energy to roll and slide so that a elevated friction and wear were established. The additional lessening of friction using nanoballs displays a guarantee in lubrication during the boundary lubrication mode.

6.1 Summary of Biofluids Properties

Nanostructured biofluids such as fullerene, hydroxylated fullerene and crown ether were added to water to create biofluids. The results showed that with the addition of solid additives, neither crown ether nor fullerene acted as abrasive as other solids in 3-body wear systems. In addition, the fullerene provided low friction and low wear, which indicates the lubrication function of this particular particle system. The hydroxylated fullerene exhibited a higher friction than fullerene, even though it is biocompatible. In contrast, the crown ether revealed elevated high friction along with elevated wear.

6.2 Contributions to Fundamental Understanding of Tribological Lubrication

This research opens a new avenue to design biofluids using nanostructured additives. Our next steps are to focus on the interactions between tissue and nanostructured additives and to develop an applicable biofluid. We will continue to test other rubbing pairs. In the human body, the cartilage has a thick and viscoelastic protein layer that maintains a certain amount of liquid for lubrication [34]. Current artificial joints are not properly lubricated and their curved surfaces can not be lubricated using conventional concepts of lubricants. Although the bio-compatibility and stability of the FU have not been studied, the methodology proposed here is promising for artificial joint lubrication.

6.3 Future Suggestions

Further understanding of interactions between fluid molecules and nanopartilces is needed in order to optimize the property. Suggestions for further research include studying the possibility of other particles for lubrication and biocompatibility and in-vitro testing toxicology tests to make sure the particles are not harmful to the body.

REFERENCES

[1] Fournier RL. Basic transport phenomena in biomedical engineering, 2nd ed. New York: Taylor and Francis; 2007. p. 93-95.

[2] Burke SR. The composition and function of body fluids, 3rd ed. St. St. Louis: The C.V. Mosby Company; 1980. p.1, 2.

[3] Rodman GP, Benedek TG, and Panetta F. The early history of synovial (joint fluids). Ann Intern Med 1995;65:821-842.

[4] Fam H, Bryant JT and Kontopoulou M. Rheological properties of synovial fluids. Biorheology 2007;44:59-74.

[5] Dumbleton JH. Tribology of natural and artificial joints. New York: Elseiver Scientific Publishing Co; 1981.

[6] Blewis ME, Nugent-Derfus GE, Schmidt TA, Schumacher BL, and Sak RL. A model of synovial fluid lubricant composition in normal and injured joints. European Cells and Materials 2007;13:26-39.

[7] Lai WM, Kuei SC, and Mow VC. Rheological equations for synovial fluids. J Biomech Eng 1998;100:169-186.

[8] McCarty DJ. Synovial fluid. Arthritis and allied conditions In: McCarty DJ and Koopman WJ eds. A textbook of rheumatology, Vol 1, 13th ed, Baltimore: Williams & Wilkins; 1997. p. 81-99.

[9] Swann DA, Silver FH, Slayter HS, Stafford W, and Shore E. The molecular structure and lubricating activity of lubricin isolated from bovine and human synovial fluids. Biochem J 1985;225:195-201.

[10] Schmid T, Lindley K, Su J, Soloveychik V, Block J, Kuettner K, and Schumacher B. Superficial zone protein (SZP) is an abundant glycoprotein in human synovial fluid and serum. Trans Orthop Res Soc 2001a;26: 82.

[11] Ogston AG and Stanier J. The physiological function of hyaluronic acid in synovial fluid: viscous, elastic and lubricant properties. J Physiol 1953;119:244-252.

[12] Mazzucco D, Scott R, and Spector M. Composition of joint fluid in patients undergoing total knee replacement and revision arthroplasty: correlation with flow properties. Biomaterials 2004;25(18):4433-4445.

[13] Schwarz IM and Hills BA. Surface-active phospholipids as the lubricating component of lubricin. B J Rheumatol 1998;37:21-26.

[14] Curtiss PH. Changes produced in the synovial membrane and synovial fluid by disease. J Bone Joint Surg 1964;46(4):873-888.

[15] Balza EA. The physical properties of synovial fluid and the special role of hyaluronic acid. In: Helfet J. ed. Disorders of the knee. 2nd ed. Philadelphia: Lippincott Co; 1982. p. 61-74.

[16] Ropes MW, Rossmcisi EC, and Bauer W. The origin and nature of normal human synovial fluid. J Clin Inves 1940;19:795-799.

[17] Sandson J and Hamermen D. Paper electrophesis of human synovial fluid. Proc Soc for Experim Biology and Med 1958;98(3):564-566.

[18] Schur PH and Sandson J. Immunological studies of the proteins of human synovial fluid. Arthritis Rheum 1963;6:15-129.

[19] Casenti G, Di Paola L, Marrelli L, and Palma MI. Rheological characterization of an artificial synovial fluid. The Int J of Artificial Org 2006;28:711-717.

[20] Todhunter RJ. Anatomy and physiology of synovial joints. In: Mcllwraith CW & Trotter GW eds. Joint disease in the horse. Philadephia: W.B. Saunders Company; 1996.

[21] Shimazu A, Jikko A, Iwamoto M, Koike T, Yan WQ, et al. Effects of HA on the release of proteoglycan form the cell matrix in rabbit chrondrocyte cultures in the presence of and absence of cytokines. Arthritis Rheum 1993;36:247-253.

[22] Mabuchi K, Fujie H, Morita M, Tsukamoto Y, Obara T, et al. The role of hyaluronic acid in articular lubrication. J. Jpn Assoc Clin Biomech 1992;14:233-236.

[23] Ghosh P, Read R, Armstrong S, Wilson D, Marshall R, et al. The effects of intra-articular administration of Hyaluronan in a model of early osteoarthritis in sheep. Arthritis Rheum 1993;22(Suppl 1):18-30.

[24] Yamamoto M , Sugarawa S, Tsukamoto Y, Motegi M, Iwata H, Ryu J, et al. Clinical evaluation of high molecular weight sodium hyaluronate (NRD101) on osteoarthritis of the knee. A phase III comparative clinical study with Artz as a control drug. Jpn Pharmacol Ther 1994;22:4059–87.

[25] Oka M and Nakumura T. Effects of high molecular weight of hyaluronic acid upon the mechanism of articular lubrication. Jpn J Articular Surg XII 3:1993;267-272.

[26] Yokobori AT, Kawaharada T, Sasaki S, Watanable S, Fang SH, et al. Mechanical test method on the estimation of the lubricant performance by hyaluronic acid. Bio-med Maters and Engr 1995;52:117-124.

[27] Dahl LB, Dahl IM, and Engstrom-Laurent L. Concentration and molecular weight of sodium hyaluronate in synovial fluid from patients with rheumatoid arthritis and other arthroplaties. Ann Rheum Dis 1985;44:817-822.

[28] Decker B, McGuckin WF, and Slocumb CH. Concentration of hyaluronic acid in synovial fluid. Clin Chem 1959;5:465-469.

[29] Balazas EA, Watson D, Duff IF, and Roseman S. Hyaluronic acid in synovial fluid. 1. Molecular parameters of hyaluronic acid in normal and arthritis human fluids. Arthritis Rheum 1967;10:357-376.

[30] Gomez JE and Thurston GB. Comparison of the oscillatory shear viscoelasticity and composition of pathological synovial fluids. Biorheology 1993;30:409-427.

[31] Prete PE, Gurakar-Osborne A, and Kashyap MI. Synovial fluid lipoproteins: review of current concepts and new directions. Semin Arthritis Rheum.1993;23:79-89.

[32] Praest BM, Greiling H, and Kock R. Assay of synovial fluid parameters: hyaluronan concentration as a potential marker for joint diseases. Clim Chim Acta 1997;266:117-128.

[33] Hall RM, Bankes MJK, and Blunn G. Biotribiology for joint replacement. Curr Orth 2001;15:281-290.

[34] Gunther RC. Lubrication, 1st ed. Chilton Book Company; Philadelphia: 1971.

[35] Dowson D. Modes of lubrication in human joints. In: Lubrication and wear in living and artificial human joints. Part 3J, Proc 1966-1967, Instn Mech Engrs 181:45-54.

[36] Schurz J, Ribitsch V. Rheology of synovial fluid. Biorheology 1987;24:385-399.

[37] Williams DF. Definitions in biomaterials. Proceedings of a Consensus Conference of the European Society for Biomaterials, Elsevier; Amsterdam: 1987.

[38] Black J. Biological performance of materials: Fundamentals of biocompatibility, 2nd ed. Troy: Marcel; 1992.

[39] Katti KS. Biomaterials in total joint replacement. Colloids and Surfaces B: Biointerfaces 2004;39:133–142.

[40] Long M. and Rack HJ. Titanium alloys in total joint replacement—a materials science perspective, Biomaterials 1998;19:1621.

[41] McKee GK and Watson-Ferrar J. Replacement of Arthritic hips by the Mckee-Farrar Prosthesis. J Bone Joint Surg Br 1966:48-B:245-259.

[42] Walker PS and Gold PL. The tribology (friction, lubrication and wear) of all-metal artificial hip joints Wear 1971;17(4)285-299.

[43] Jin ZM. Analysis of mixed lubrication mechanism in metal-on-metal hip joint replacements, Proc Instn Engrs Part H: J Engineering in Medicine, Tech Note 2002; 216:A85-90.

[44] McKellop H, Park SH, Chiesa R, Doorn P, and Lu B. In vivo wear of 3 types of metal-on-metal hip prostheses during 2 decades of use. Clin Orthop (Suppl.) 1996; 29S:128–140.

[45] Chan FW, Bobyn JD, Medley JB, Krygier JJ, and Tanzer M. The otto Au frame award-wear and lubrication of metal-on-metal hip implants. Clin Orthp Related Res 1999; 369:10-24.

[46] Davidson JA and Georgette FS. State-of-the-Art Materials for orthopaedic Prosthetic Devices: on Implant Manufacturing and Material Technology. Proc Soc of manufacturing Engineering, Itasca, IL.

[47] Buford A, Goswami T. Review of wear mechanisms in hip implants: Paper I – General. Mater and Des 2004;25:385-393.

[48] Biomet, Inc., Warsaw, IN. Addressing osteolysis in total hip arthroplasty. Form No. Y-BEM-052/071594/HP; 1994

[49] Szycher M. Biocompatible polymers, metals and composites. Lancaster: Technomic Publ; 1983. p. 1071.

[50] Wang A, Essner A, and Klein R. Effects of contact stress on friction and wear of ultra high molecular weight polyethylene. J Engl Med 1995;215(5):133-139.

[51] Ramakrishna S, Mayer JE, Wintermantel, and Leong KW. Biomedical applications of polymer-composite materials: a review. Comp Sc Technol 2001;61(9):1189.

[52] Schmitt FO. Adventures in molecular biology. Ann. Rev. Biophys and Biophys Chem 1985;14:1-22.

[53] Garino P. Modern ceramic-on-ceramic total hip systems in the United States. Early results. Clin Orthop Rel Res 2000;379, 41–47.

[54] Hannouche D, Hamadouche M, Nizard R, Bizot P, Meunier A, and Sedel L. Ceramics in total hip replacement. Clin Orthop Rel Res 2005;430:62–71.

[55] Sedel L, Nizard R, Bizot P, and Meunier A. Perspective on a 20-year experience with ceramic-on-ceramic articulation in total hip replacement. Seminar Arthroplasty 1998;9(2):123–134.

[56] Akagi M, Nakamura T, Matsusue Y , Ueo T, Nishijyo K, and Ohnishi E. The bisurface total knee replacement: A unique design for flexion. forty-nine-year follow-up study. J Bone Joint Surg Am 2000;82(11):1626–1633.

[57] Oonishi H, Aono M, Murata N, and Kushitani S. Alumina versus polyethylene In: Total knee arthroplasty. Clin Orthop Rel Res 1992;282:95–104.

[58] Yasuda K, Miyagi N, and Kaneda K. Low friction total knee arthroplasty with the alumina ceramic condylar prosthesis. Bull Hosp Joint Dis 1993;53(2):15–21.

[59] Mohamed N, Rahaman MN, and Yao A. Ceramics for prosthetic hip and knee joint replacement. J Am Ceram Soc 2007;90(7):1965–1988.

[60] Skinner B. Ceramic bearing surfaces. Clin Orthop Rel Res 1999:369:83–91.

[61] Skotheim JM and Mahadevan L. Soft lubrication: the elastohydrodynamics of nonconforming and conforming contacts. Phys of Fluids 2005;17(9):1-24.

[62] Grodzinsky AJ, Lipshitz H, and Glimcher MJ. Electromechanical properties of articular cartilage during compression and stress relaxation. Nature 1978;275(5679): 448-450.

[63] Mow VC and Guo XE. Mechano-electrochemical properties of articular cartilage: their inhomogeneities and anisotropies. Annu Rev Biomed Eng 2002;4:175.

[64] Mow VC, Holmes MH, and Lai MW. Fluid transport and mechanical properties of articular cartilage: a review. J Biomech 1984;17:377.

[65] Damiano R, Duling BR, Ley K, and Skalak TC. Axisymmetric pressure-driven flow of rigid pellets through a cylindrical tube lined with a deformable porous wall layer. J Fluid Mech 1996;314:163.

[66] Feng J and Weinbaum S. Lubrication theory in highly compressible porous media: The mechanics of skiing, from red cells to humans. J Fluid Mech 2000;422:281-317.

[67] Fitzgera JM. Mechanics of red-cell motion through very narrow capillaries. Proc R Soc London Ser B 1969;174(1035):193.

[68] Lighthill MJ. Pressure-forcing of tightly fitting pellets along fluid-filled elastic tubes. J Fluid Mech 1968;34:113-143.

[69] Secomb TW, Hsu R, and Pries AR. A model for red blood cell motion in glycocalyx-lined capillaries. Am J Physio 1998;274(3):H1016-H1022.

[70] Secomb W, Skalak R, Özkaya N, and Gross JF. Flow of axisymmetric red blood cells in narrow capillaries. J Fluid Mech 1986;163:405-423.

[71] Tözeren H and Skalak R. The steady flow of closely fitting incompressible elastic spheres in a tube. J Fluid Mech 1978;87:1-16.

[72] Wang W and Parker JH. The effect of deformable porous surface layers on the motion of a sphere in a narrow cylindrical tube. J Fluid Mech 1995;283:287.

[73] Weinbaum S, Zhang X, Han Y, Vink H, and Cowin S. Mechanotransduction and flow across the endothelial glycocalyx. Proc Nat Acad Sci USA 2003;100:7988.

[74] Tanner RI. An alternative mechanism for the lubrication of synovial Joints. Phys Med Biol 1966;11:119.

[75] Martin A, Clain J, Buguin A, and Brochard-Wyart F. Wetting transitions at soft, sliding interfaces. Phys Rev E 2002;65:031605.

[76] Klein J, Perahia D, and Warburg S. Forces between polymer-bearing surfaces undergoing shear. Nature 1991:352:143-145.

[77] Sekimoto K and Leibler L. A mechanism for shear thickening of polymer-bearing surfaces: elasto-hydrodynamic coupling. Europhys Lett 1993;23:113.

[78] Abkarian M, Lartigue C, and Viallat A. Tank treading and unbinding of deformable vesicles in shear flow: determination of the lift force. Phys Rev Lett 2002;88:068103.

[79] Beaucourt J, Biben T, and Misbah C. Optimal lift force on vesicles near a compressible substrate. Europhys Lett 2004;67:676.

[80] McCutchen WC. The frictional properties of animal joints. Wear 1962; 5: 1-17.

[81] McCutchen CW. Lubrication of joints, the joints and synovial fluid. New York: Academic Press; 1978.

[82] Dowson D, Unsworth A, and Wright V. Analysis of 'boosted lubrication' in human joints. J Mech Eng Sci 1970;12:364.

[83] Ateshian GA, Wang H, and Lai WM. The role of interstitial fluid pressurization and surface porosities on the boundary friction of articular cartilage. J. Tribol 1998;120(2):241.

[84] Hodge WA, Fijiann RS, Carlson KL, Burgess RG, Harris WH, and Mann RW. Contact pressures in the human hip joint measured in vivo. Proc Nat. Acad Sci U. S. A. 1986;83:2879.

[85] Grodzinsky AJ. Electromechanical and physicochemical properties of connective tissue. Crit Rev Anal Chem 1985;9:133.

[86] Buschmann MD and Grodzinsky AJ. A molecular model of proteoglycan-associated electrostatic forces in cartilage mechanics. J. Biomech. Eng., 1995;117:179.

[87] Wojtys EM and Chan DB. Meniscus structure and function. Instr. Course Lect. 2005;54:323.

[88] Presson BNJ. Sliding friction: physical principles and applications, NanoScience and Technology Series, 2nd ed., Berlin: Springer, 1998.

[89] Fung YC. Biomechanics: mechanical properties of living tissues. 2nd ed. New York: Springer-Verlag; 1993.

[90] Fox B, Taylor N, and Yazdany J. Appendix a- glossary. In: Arthritis for dummies. 2nd ed., Hoboken NJ: Wiley Publishing Inc; 2004. p.319.

[91] Pearle AD, Warren RF, Rodeo SA. Basic science of articular cartilage and osteoarthritis. Clin Sports Med 2005;24:(1):1.

[92] Stedman's Medical Dictionary, 24th ed. J.V. Basmajian et al. eds. Baltimore: Williams & Wilkins; 2004. p.1002.

[93] Sawae Y, Murakami T, and Chen J. Effects of synovia constituents on friction and wear of ultra high molecular weight polyethylene (UHMWPE) sliding against prosthetic joint materials. Wear 1998;216:213–9.

[94] Bos MA and van Vliet T. Interfacial rheological properties of adsorbed protein layers and surfactants: a review. Adv Colloid Interface Sci 2001;91:437–471.

[95] Kirk P. Physical properties of synovial fluid: composition, rheology and lubrication properties. Report No. M5874. Winterthur: Sulzer Orthopedics; 1997.

[96] National Institutes of Health National Institute of Arthritis/6Muscoskeletal and Handbook of Health, Osteoarthritis, 1998:3.

[97] Carter DR and Beaupre GS. Skeletal function and form, Cambridge University Press; Cambridge: 2001.

[98] Snibble JC and Gambardella RA. Use of injections in joints and sports activity. Clin Sports Med 2005;24:83-91.

[99] Hollander JL and Brown EM. Comparative effects of and use of hydrocortisone as a local antiarthritc agent. JAMA 1952;147:629-635.

[100] Waseem M, Sadiq S, Gambhir AK, Lim J, Maxwell S, et al. Safety and efficacy of intra-articular injection of the hip. Hip International 2002;12:378-382.

[101] Flanagan J, Casale FF, Thomas TL, and Desai KB. Intra-articular injection for pain relief in patients awaiting hip replacement. Annals of the Royal College of Surgeons 1988;70(3):156-157.

[102] Karuppiah SV and Gibson P. The safety of hip injection with cortisteroid in the diagnosis and treatment of osteoarthritis. Hip International 2007;17(1):36-39.

[103] Kingston B. Understanding joints, a practical guide to their structure and function. Stanley Thornes (Publisher) Ltd; London: 2000. p. 9.

[104] Enderle J, Blanchard S, and Bronzino J. Introduction to biomedical engineering ElsevierAcademic Press; Boston: 2001. p.65.

[105] McKee GK. Development of total hip joint replacement in: Lubrication and wear in living and artificial human joints, 1966-1967, Part 3 Proc Instn Mech. Engrs 181:85.

[106] Charnley J. Arthroplasty of the hip,a new operation. Lancet 1961;1:1129-1132.

[107] Mohsen M. An UHMWPE homocomposite for joint prostheses In: Jacobs JJ, Craig TL, editors. Alternating bearing surfaces in total joint replacement. West Conshohocken:1998. p. 256.

[108] Berry DJ, Harmsen WS, Cabanela ME, and Morrey BF. Twenty-five-year survivorship of 2000 consecutive primary charnley total hip replacements. J Bone Jt Surg 2002;84A(2):171-177.

[109] Burger NDL, Vaal de PL, and Meyer JP. Failure analysis on retrieved ultra high molecular weight polyethylene (UHMWPE) acetabular cups. Engr Failure Analysis 2007;14:1329-1345.

[110] Mallchau H, Herberts P, Garellick G, So¨derman P, and Eisler T. Prognosis of total hip replacement, update of results and risk ratio, analysis for revision and re-revision. Swedish National Hip Arthroplasty Register; 2000. p.1979–2000.

[111] Huo MH and Cook SM. What's new in hip arthroplasty. J Bone Joint Surg 2001;83A(10):1598–610.

[112] Davidson D, Graves S, Batten J, Cumberland W, Fraser J, and Harris J, et al. Australian Orthopaedic Association National joint replacement registry. Annual Report; Australia; 2002.

[113] Bauer LA, Birenbaum NS, and Meyer GJ. Biological applications of high aspect ratio nanoparticles. J Mater Chem 2004;14:517-526.

[114] Polyscience Inc. www.polyscience.com.

[115] Dynal Biotech. www.dynalbiotech.com.

[116] Dubertret B, Skourides P, Norris DJ, Noireaux V, Brivanlou AH, and Libchaber A. In vivo imaging of quantum dots encapsulated in phospholipid micelles. Science 2002;298:1759.

[117] Bakunin VN, Suslov AY, Kuzmina GN, and Parenago OP. Synthesis and application of inorganic nanoparticles as lubricant components – a review. J Nano Res 2004;6(2-3):273-284.

[118] Zhang Z, Xue Q, and Zhang J. Synthesis, structure and lubricating properties of dialkylidithiophosphate-modified Mo-S compound clusters. Wear 1997;209:8-12.

[119] Rapoport L, Billik Y, Feldman Y, Homoyonfer M, Cohen SR, and Tenne R. Hollow nanopartilces of WS_2 as potential solid-state lubricants. Nature 1997;387:791-793.

[120] Baker IL, Singletary CR, and Solomon EM. Neutral and basic sulfonates. Ing Eng Chem 1954:46:1035-1042.

[121] Dutta J, Hofmann H, Hollenstein C, and Hofmeister H. Plasma-produced silicon nanoparticle growth and crystallization processes. In: Fendler JH ed. Nanoparticles and nanostructured films, preparation, characterization and application, NewYork: Wiley-VCH; 1998. p. 177, 178.

[122] Dutta J, Reaney M, Bossel C, Houriet R, and Hofmann H. Nanostructured Materials 1995;6:493-496.

[123] White LT. A case study of technological innovation. Its context and tradition. Technology and Culture 1961;2 (2):97-111.

[124] Zhang ML, Ding GL, Jing XY, and Hou XQ. Preparation, modification and application of nanoscale SiO_2. Appl Sci Technol 2004;31(6):64-66.

[125] Li XH, Sun R, Zhang ZJ, and Dang HX. Problems of polymer/inorganic nanocomposition by chemical bonds. Prog Nat Sci 2004;14:1.

[126] Ke YC. Polymer-inorganic nano-composites. Beijing: Chemistry Industry Press; 2002.

[127] Li ZW and Zhu YF. Surface-modification of SiO2 nanoparticles with olic acid. Applied Surface Science 2003;211(1-4):315-320.

[128] Li Xiaohong, Cao Zhi, Zhang Zhijun, and Dang Hongxin. Surface-modification insitu of nano-SiO_2 and its structure and tribological properties. Applied Surface Science 2006; 252:7856-7861.

[129] Battez Hernandez A, Fernandez Rico J.E, Navas Arias A, Viesca Rodriguez J.L, Chou Rodriguez R, et al. The tribological behavior of ZnO nanoparticles as an additive to PAO6. Wear 2006;261:256-263.

[130] Fernandez Rico JE, Hernandez A, and Cuervo Garcia D. Wear prevention characteristics of binary oil mixture. Wear 2002;253:827-831.

[131] Masjuhi HH and, Maleque MA. Investigation of the anti-wear characteristics of palm oil methyl ester using a four-ball tribotester test. Wear 1997;206:179-186.

[132] Spikes HA. Film-forming additives–direct and indirect to reduce friction. In: Proceedings of the 12th International Colloquium Tribology 2000-Plus; Esslingen: 2000. p. 2045-2054.

[133] Guangteng G and Spikes H. The control of friction by molecular fractionation of base fluid mixtures in metal surfaces. Tribol Trans 1997;40(3):461-469.

[134] Kolodziejcjczyk L, Martinez-Martinez D, Rojas TC, Fernandez A, and Sanchez-Lopez JC. Surface modified Pd nanoparticles as superior additive for lubrication. J Nanoparticle Res 2007;9:639-645.

[135] Krastev I, Petkova N, and Zielonka A. Properties of silver-antimony alloys electrodeposited from ferrocyanide-thiocyanate electrolytes. J Appl Electrochem 2002;32(7):811-818.

[136] Subramonian B, Kato K, Adachi K, and Basu B. Experimental evaluation of friction and wear properties of solid lubricant coatings on SUS440C steel in liquid nitrogen. Tribol Lett 2005;20(3-4):263-277.

[137] Jayaram G, Marks LD, and Hilton MT. Nanostructures of Au-20%Pd layers in MoS_2 multilayers solid lubricant films. Surf Coat Technol 1995;77(1-3):393-399.

[138] Antler M. Electrical contact (Ed. Slade PG). Marcel Dekker, New York, p. 179-202.

[139] Askeland DR and Phule PP. The science and engineering of materials. 4th edn. Pacific Grovel: Brooks/Cole; 2003. p. 626.

[140] Radice S and Mischler S. Effect of and mechanical parameters on the lubrication behavior of Al_2O_3 nanoparticles in aqueous suspensions. Wear 2006; 261:1032-1041.

[141] Dowson D, Priest M, Dalmaz G, and A A Lubrecht AA. Symposium on tribology. In: Proceedings of 31st leeds-lyon September 7-10 2004. Trib and Interface Engr Series 2005;48:3-909.

[142] Chakravorty D and Giri AK. Nanomaterials, chemistry for the 21st century. In: Rao CNR ed.. Chemistry of advanced materials. Oxford: Blackwell; 217.

[143] Schuberf U, Tewinel S, and Lamber R. Metal complexes in inorganic matrixes.15. Coordination of metal ions by lysinate-modified titanium and zirconium alkoxides and the preparation of metal/titania and metal/zirconia nanocomposites. Chem Mater 1996;8:2047.

[144] Shea KJ, Loy DA, and Webster O. Arylsilsesquioxane gels and related materials. New hybrids of organic and inorganic net. J Am Chem Soc 1992;114:6700.

[145] Monkikawa A, Lyoka Y, Kakimoto M, and Lmai Y. Preparation of new polyimide–silica hybrid materials via the sol–gel process. J Mater Chem 1992;2:679.

[146] Zhang Z, Zhang J, and Xue Q. Study on the structure of surface-modified MoS_2 nanoparticles. Phys Chem 1994;98:12973.

[147] XueQ, Liu W, and Zhang Z.Friction and wear properties of a surface-modified TiO2 nanoparticle as an additive in liquid paraffin. Wear 1997;213:29-32.

[148] Dellacorte C and Fellenstein J. Preparation and tribological properties of tetrafluorobenzoic acid-modified TiO_2 nanoparticles as lubricant additives Tribol Trans 119;40(4):639-642.

[149] Lu JJ, Xue QJ, and Ouying JI. Thermal properties and tribological characteristics of CeF3 compact. Wear 1997;211:9-14.

[150] Xue QJ and Lu JJ. Sliding friction, wear and oxidation behavior of CeF_3 compact in sliding against steels at temperatures to 700 ^{o}C in air. Wear 1998;219:73-77.

[151] Lu JJ, Xue QI, and Zhang W. Effect of silver on the sliding friction and wear behavior of CeF_3 compact at elevated temperatures. Wear 1998;214:107-111.

[152] Feng DP, Zhou JF, Lin WM, and Xue QJ. Preparation and tribological properties of tetrafluorobenzoic acid-modified TiO_2 nanoparticles as lubricant additives. Wear 2000;246:68-73.

[153] Zhou JF, Wu ZS, Zhang ZJ, Liu WM, and Dong HX. Study on an antiwear and extreme pressure additive of surface coated LaF_3 nanoparticles in liquid paraffin. 1998;249:333-337.

[154] Hu ZS and Dong IX. Study on anti-wear and reducing friction additive of nanometer titanium oxide. Wear 1998;216:92-96.

[155] Gao YJ, Sun R, Zhang Z, and Xue Q. Tribological properties of oleic acid - modified TiO_2 nanoparticle in water. Mater Sci Eng 2000;A286:149-151.

[156] Ye W, Cheng T, Ye Q, Guo X, Zhang Z, and Dang H. Preparation and tribological properties of tetrafluorobenzoic acid-modified TiO2 nanoparticles as lubricant additives. Materls Sci and Engr 2003;A359:82-85.

[157] Jost HP. Tribology: the first 25 years and beyond achievements shortcomings and future tasks. Ind Lubr Triob 1992;44:22-27.

[158] Sliney HE. Rare earth fluorides and oxides – an exploratory study of their use as solid lubricants at temperature to 1800F, NASA, Washington, DC: NASA TN-D-531;1969.

[159] Dumdum JM, Aldorf HE, and Barnum EC. Lubricant additive for grease, paste and suspension. NLGI spokesman 1984;48(4):111,

[160] Aldorf HE. Rare earth halide grease compositions, US Patent No. 4,507,214, 1985.

[161] Lian YF, Xue QJ, Zhang XH, and Wang HQ. The mechanism of synergism between ZDDP and CeF_3 additives. Lubr Sci 1995;7(2):261-272.

[162] Sunqing Q, Junxiu D, and Guoxu C. Tribological properties of CeF_3 nanoprticles as additives in lubricating oils. Wear 1999;230:25-38.

[163] Bhat VS. Biomaterials, Boston: Kluwer Academic Publishers and Norosa Publishing House; 2002. (Biomaterials in total joint replacement for table in thesis)

[164] Donachie MJ. Titanium: A technical guide. Metals Park, OH: ASM International; 1998. p.1-4.

[165] Boyer R, Welsch G, and Collings E eds. Materials properties handbook: titanium alloys. Metals Park, OH: ASM International; 1994. p. 3-11.

[166] Petersen DW, Lemmons JE, and Lucas LC. Comparative evaluations of surface characteristics of cp titanium, Ti-6Al-4V and Ti-Mo-2.8Nb-0.2 Si. In: Symposium on titanium, niobium, zirconium, and tantalum for medical and surgical applications. J ASTM Internat 2004;2(3):151,152.

[167] Arsenjev AP, Arsenjev PA, Evdokimov AA, Makaricheva EU, and Sheinin MJ. The processing of surgical implants from pure titanium. Krasnokazarmennaja str., 14, Moscow, 11 1250 Russia, 384,385,

[168] World Health Organization. Hygienic criteria of environment conditions, 24, Titanium, Geneva; 1986.

[169] Niiomi M. Recent metallic materials for biomedical applications. Met Mater Trans A 2002;33:477-486.

[170] Fraker AC. Corrosion of metallic implants and prosthetic devices. In: Metals handbook. Metals Park, OH: ASM International;1997.

[171] Zitter H and Plenk H. The electrochemical behavior of metallic implant materials as an indicator of their biocompatibility. J Biomed Maters Res 1987;21:881-896.

[172] Williams DF. Titanium and titanium alloys. In: Williams DF, ed. Biocompatibility of clinical implant materials, Boca Raton, Florida: CRC Press;1981.

[173] Turner TM, Summer DR, Urban RM, Igloria R, and Galante JO. Maintenance of proximal cortical bone with use of a less stiff femoral component in hemiarthroplasty of the hip without cement: An investigation in a canine model at six months and two years. J Bone Joint Surg Am 1997;79:1381-1390.

[174] Woo SL, Lothringer KS, Akeson WH, Coutts RD, Woo YK, Simon BR, and Gomez MA. Less rigid internal fixation plates; historical perspectives and new concepts. J Orth Res 1984;1:431-449.

[175] Freese AL, Volas MG and Wood JR. Metallurgy and technological properties of titanium and titanium alloys. In: Brunette DM, Tengall P, Textor M, and Thomson P, eds. Titanium in medicine. Berlin: Springer; 2001. p. 31.

[176] Davidson JA, Georgette FS. State-of-the-Art Materials for Orthopaedic Prosthetic Devices: In: Jacobs JJ and Craig TL, eds. Alternative bearing surfaces in total joint replacement, ASTM STP 1346: 1998 .

[177] Callister WD. Material Science and Engineering: An introduction. New York: John Wiley & Sons; 2002. p. A5-A8.

[178] Buckwalter JA. Regenerating articular cartilage: why the sudden interest? Orthop Today 1996;16:4-5.

[179] Kroto HW, Heath JR, O'Brien SC, Curl RF, and Smalley RE. C_{60}: buckminsterfullerene. Nature 1985;318:162-163.

[180] Kratschmer W, Fostiropoulos K, and Huffman DR. The infrared and ultraviolet absorption spectra of laboratory-produced carbon dust: evidence for the presence of the C_{60} molecule. Chem Phys Lett 1990;170:167-170.

[181] Kratschmer W, Lamb LD, and Fostiropoulos K. Solid C60: a new form of carbon. Nature 1990;347:354-358.

[182] Yan Feng-yuam and Xue Quin-ji. The antifriction behaviors of C_{60}/C_{70}. J Phys D Appl. Phys 1997;30:781-786.

[183] Bhustan B, Gupta BK, Van Cleef W, Capp C, and Coe JV. Sublimed C60 films for tribology. Applied Physics Letters 1993;62(25):3253-3255.

[184] Gupta BK and Bhushan B. Fullerene particles as an additive to liquid lubricants and greases for low friction and wear. Lubrication Engineering 1994;50(7):524-528.

[185] Ginzburg BM, Kireenko OF, Shepelevskh AA, Shibaev LA, Tochilnikov DG, and Leksovskii AM. Thermal and tribological properties of fullerene-containing composite systems. Part 2. formation of tribo-polymer films during boundary sliding friction in the presence of fullerene C_{60}. Part B, Physics 2005;44:93-115.

[186] Feng B. Relationship between the structure of C_{60} and its lubricity: A review. Lubr Sci 1997;92:181-193.

[187] Bhushan B, Gupta BK, Van Cleef GW, Capp C, and Coe JV. Fullerene (C_{60}) films for solid lubrication. Tribol Trans 1993;36(4):573-580.

[188] Blau PJ and Haberlin CE. An investigation of the microfrictional behavior of C_{60} particle layers on aluminum. Thin solid films 1992;219:129-134.

[189] Gupta BK, Bhushan B, and Capp C. Materials characterization and effect of purity and ion implantation on the friction and wear of sublimed fullerene films. J Mater Res 1994;9:2823.

[190] Gui-Chang J, Wen-Chao G, and Zheng Qi-Xin Z. Synthesis of fullerene-acrylamide copolymer nanoball and its lubrication properties. Chinese Journal of Chemistry 2004;22:877-881.

[191] Bosi S, Da Ros T, Spalluto G, and Prato M. Fullerene derivatives: an attractive tool for biological applications. Eur J Med Chem 2003;38, 913–923.

[192] Dugan LL, Turetsky DM, Du C, Lobner D, Wheeler M, Almli CR, Shen C K, Luh T, Choi DW, and Lin TS. Carboxyfullerenes as neuroprotective agents. Proc Natl Acad Sci U.S.A. 1997;94:9434–9439.

[193] Lotharius J, Dugan LL, and O'Malley KL. Distinct mechanisms underlie neurotoxin-mediated cell death in cultured dopaminergic neurons. J Neurosci 1999;19: 1284–1293.

[194] Dugan LL, Gabrielsen JK, Yu SP, Lin TS, and Choi DW. Buckminster fullerenol free radical scavengers reduce excitotoxic and apoptotic death of cultured cortical neurons. Neurobiol Dis 1996;3:129–135.

[195] Jin H, Chen WQ, Tang XW, Chiang LY, Yang CY, Schloss JV, and Wu JY. Polyhydroxylated C_{60}, fullerenols, as glutamate receptor antagonists and neuroprotective agents. J Neurosci Res 2000;62:600–607.

[196] Chen YW, Hwang KC, Yen CC, and Lai YL. Fullerene derivatives protect against oxidative stress in RAW 264.7 cells and ischemia-reperfused lungs. Am. J. Physiol. Regu Integr Comp Physiol 2004;287, R21–R26.

[197] Bogdanovic G, Kojic V, Dordevic A, Canadanovic-Brunet J, Vojinovic-Miloradov M, and Baltic VV. Modulating activity of fullerol $C_{60}(OH)_{22}$ on doxorubicin-induced cytotoxicity. Toxicol In Vitro 2004;18, 629–637.

[198] Lu LH, Lee YT, Chen HW, Chiang LY, and Huang HC. The possible mechanisms of the antiproliferative effect of fullerenol, polyhydroxylated C_{60}, on vascular smooth muscle cells. Br J Pharmacol 1998;123, 1097–1102.

[199] Isakovic A, Markovic Z, Todorovic-Markovic B, Nikolic N, Vranjes-Djuric S, et al. Distinct cytotoxic mechanisms of pristine versus hydroxylated fullerene. Toxicological Sciences 2006;(91)1:173-183.

[200] Cheng X, Kan AT, and Tomson M B. Naphthalene adsorption and desorption from aqueous C_{60} fullerene. J Chem Eng Data 2004;49:675–683.

[201] Deguchi S, Rossitza, GA, and Tsujii K. Stable dispersions of fullerenes, C_{60} and C_{70} in water, preparation and characterization. Langmuir 2001;17(19):6013-.6017.

[202] Sayes C, Fortner J, Lyon D, Boyd A, Ausman K, Tao Y, Sitharaman B, Wilson L, West J and Colvin VL. The differential cytotoxicity of water soluble fullerenes. Nano Lett 2004;4;1881–1887.

[203] Oberdorster E. Manufactured nanomaterials (fullerenes, C_{60}) induce oxidative stress in the brain of juvenile largemouth bass. Environ Health Perspect 2004;112:058–1062.

[204] Pederson CJ. Cyclic polyethers and their complexes with metal salts. J Am Chem Soc 1967;89:7017.

[205] a) Pedersen CJ, Lehn JM, and Cram DJ. Crowns and crypts: a fascinating group of multidentate macrocyclic ligands. Reasonance 2001;6:71 b) Lehn JM. Supramolecular chemistry-concepts and perspectives. Angew Chem 1998;100:91; c) Cram DJ. Angew Chem 1988;100:1041; Angew Chem Int Ed Eng 1988;27:1009. d) Pedersen CJ. Angew Chem 1988;100:1053; Angew Chem 1987;27:1021.

[206] Gokel GW, Leevy WM, and Weber ME. Crown Ethers: Sensors for ions and molecular scaffolds for materials and biological models. Chem Rev 2004;104:2723-2750.

[207] Pederson CJ. Cyclic polyethers and their complexes with metal salts. J Am Chem Soc 1967;89:7017.

[208] Liotta CL and Berknerin, J. 18-Crown-6 in encyclopedia of reagents for organic synthesis. Paquette L, ed., New York: J. Wiley & Sons; 2004.

[209] Wang A, Polineni VK, A. Essner, Stark C, and Dumbleton JH. Lubrication and wear of ultra-high molecular weight polyethylene in total joint replacements. Trib Intern 1998;31(1-3):17-33,

[210] Clarke IC, Chan FW, Essner A, Good V, Kaddick C, Lappalainen R, Laurent M, McKellop H, McGarry W, Schroede D, Selenius M, Shen MC, Ueno M, Wang A, and Yao JQ. Multi-laboratory simulator studies on effects of serum proteins on PTFE cup wear. Wear 2001;250:188–198.

[211] Liao YS, Benya PD, and McKellop HA. Effect of protein lubrication on the wear properties of materials for prosphetic joints. J Biomed Mater Res Appl Biomater 1999;48:465–473.

[212] Yao JQ, Laurent MP, Gilbertson LN, Blanchard CR, Crowninshield RD, and Jacobs J . A Comparison of biological lubricants to bovine calf serum for total joint wear testing. Ortho Res Soc 2002, Sect 2, p. 1004.

[213] Yao JQ, Laurent MP, Johnson CR, and Crowinsheild RD. The influences of lubricant and material on polymer/CoCr sliding friction. Wear 2003;255:780–784.

[214] Kokubo T, Kushitani H, and Sakka S. Solutions able to reproduce in vivo surface-structure changes in bioactive glass-ceramic A-W. J Biomed Mater Res 1990;24:721-734.

[215] Shi XF. Apatite coating over zirconium metal by a biomimetic method. Master's thesis, Terre Haute, IN: Rose-Hulman Institute of Technology; 2002.

[216] Mow VC, Ratcliffe A, and Poole AR. Cartilage and diarthrodial joints as paradigms for hierachical materials and structures. Biomaterials 1992;13(2):67-97.

[217] Polymer Nano Composite lab, Texas A&M University, http://www1.mengr.tamu.edu/PolymerNanoComposites/index.html (access date:01/15/2008).

[218] Microscopy and Imaging center, Texas A&M University, http://www.tamu.edu/mic/ (access date: 03/08/2008).

[219] Ribeiro R. A tribological and biomimetric study of potential bone repair materials. Ph.D. dissertation 2006, Texas A&M University, United States – Texas. Retrieved August 3, 2008, from Dissertation and Theses @ Texas A&M System database (Publication No. AAT 3296524).

[220] Chescoe D and Goodhew PJ. The operation of transmission and scanning electron microscopes. New York: Oxford University Press; 1990. p.3.

[221] Conrad BP et.al. Can synovial fluid viscosity be used as a physical marker for osteoarthritis? Key Biscayne, Florida; Summer Bioengineering Conference, June 25-29, 2003.

[222] Lumsden JM. Apparent viscosity of the synovial fluid from mid-carpal, tibiotarsal, and distal interphalangeal joints of horses. Amer J of Vet Res 1996;57(6):879-883.

[223] Wright V and Dowson D. Lubrication and cartilage. J Anat 1976;121(1):107-118.

[224] Levine MG and Kling DH. Rheologic Studies of synovial fluid. J Clin Investig 1956;35(12):1419-1427.

[225] Davies DV and Palfrey AJ. Physical properties of synovial fluid. In: Lubric. Wear and Joints. Wright V, ed., London: Sector; 1969. p. 20-28 .

[226] Vos R and Theyse F. Lubricating properties of synovial fluid in human and animal joints. In: Wright V, ed., Lubrication and wear in joints. London: Sector; 1969. p. 29-34.

[227] Anderson P. Water-lubricated pin-on-disc tests with ceramics. Wear, 1992;154(1):37-47.

[228] Sasaki S. The effects of water on friction and wear of ceramic. J of Jpn Soc of Lubr Eng 1988;33(8) 620-628 (in Japanese).

[229] Zum Gahr KH. Sliding wear of ceramic/ceramic, ceramic/steel and steel/steel pairs in lubricated and unlubricated contact. Wear1989;133(1):1-22.

[230] Fischer TE, Anderson MP, Jahanmir S, and Salher R. Friction and wear of tough and brittle zirconium in nitrogen, air, water, hexadecane and hexadecane containing stearic acid. Wear 1988;124(2):133-148.

[231] Horton S, Dowson D, Riley F, and Wallbridge N. The sliding wear behaviour of nonoxide ceramics. In: Proc. 2nd Znt. Symp on ceramic materials and components for enghes, Liibeck-Travemiinde, April 14-17, 1986, Verlag Deutsche Keramische Gesellschaft, Bad Honnef; 1986:759-765.

[232] Tomizawa H and Fischer T. Friction and wear of silicon nitride and silicon carbide in water: hydrod~amic lubrication at low sliding speed obtained by tribochemical wear. Am Soc Lubr Eng Trans 1987;30(1):41-46.

[233] Gates R, Hsu S and Klaus E. Tribochemical mechanism of alumina with water, Sot. Trib. Lubr. Eng. Trans., 32 (3) (1989) 357-363.

[234] Nieminen I, Andersson P and Hohnberg K. Friction measurement by using a scratch test method, Wear, 130 (1989) 167-178.

[235] Andersson P and YiCistalo O. The influence of lubrication on ceramic and steel sliding contacts, Mater. Sci. 1989;A109:407-413.

[236] Wright KWJ, Dobbs HS, and Scales JT. Wear studies on prosthetic materials using the pin-on-disc. Biomaterials 1982;3:41–48.

[237] Hun Z., Su SH, and Zhang JH. Tribological study on new therapeutic bionic lubricants. Tribo Lett 2007;28:51-58.

[238] Yao JQ, Laurent MP, Gilbertson LN, Blanchard CR. Crowninshield RD, and Jacobs JJ. A comparison of biological lubricants to bovine calf serum in total joint wear testing. 48th Annual Meeting of the Orthopaedic Research Society S, Dallas, TX ; 2002:294.

[239] Saarri H, Santavira S, Nordstrom D, Paavolainen P, and Konttinen YT. Hyaluronate in total hip replacements. J Rheomatol 1993;20:87-90.

[240] Delecrin J, Oka M, Takahashi S, Yamamuro T, and Nakamura T. Changes in joint fluid after total arthroplasty. Clin Ortho Relat Res 1994;307:240-249.

[241] Burger NDL, de Vaal P.L., and Meyer JP. Failure analysis on retrieved ultra high molecular weight polyethylene (UHMWPE) acetabular cups. Engr Failure Ana 2007;1:1329-1345.

[242] Brauman JI and Szuromi P. Thin films. Science 1996;273:855.

[243] Hwang Y, Park H.S, Lee JK, and Jung WH. Thermal conductivity and lubrication characteristics of nanofluids. Current Applied Physics 2006;6S1:e67–e71.

[243] Wasan DT and Hikolow AD. Spreading of nanofluids on solids. Nature 2003:423:156-159.

[244] Ohsuk N and Murakami T. Frictional behavior of some knee prostheses. In: Proceedings of Japanese International Tribology Conference. Nagoya 1990:713-718.

[245] Dowson D and Wright V. Lubrication friction and wear in total hip replacement. In: Proceedings Fifth International Symposium on Orthopaedic Surgery. Nymegan; 1972:127-143.

[246] Ginzburg BM, Kireenko OF, Tochil'nikov DG, and Bulaiov VP. Formation of wear-resistant structure by sliding friction of steel on copper in the presence of fullerene or fullerene soot. Tech Phys Lett 1995;21(12):966-967.

[247] Boyer R, Welsch G, and Collings EW, eds. Materials properties handbook: titanium alloys. Metals Park, OH: ASM International; 1995.

[248] Gokel GW. Crown ethers and cryptands. Cambridge, England: Royal Society of Chemistry; 1991.

[249] Kajdas C, Harvey SSK, and Wilusz, E. Encyclopedia of tribology. New York: Elsevier; 1990.

[250] Ribeiro R, Ganguly P, Darensbourg D, Usta, M, Ucisik AH, and Liang H. Biomimetic study of a polymeric composite material for joint repair applications. J Matls Res 2007;22(6):1632-1639.

[251] Umetani S, Tsurubou S, Takayuki S, and Komatsu Yu. Macrocyclic ligand as ion size selective masking reagent in metal ion separation. RIKEN Review No. 35 (May, 2001): Focused on New Trends in Bio-Trace Elements Research.

[252] Junko Morita, Shinji Tsuchiya, Nao Yoshida, Nirei Nakayama, Sayaka Yokokawa, and Shojiro Ogawa. The unique properties observed for the unsymmetrical macrocyclic compounds with the highly distorted structure. Tetrahedron 2007;63(38):9522-9530.

[253] Kohno H and Tekeda S. Chains of crystalline-Si nanospheres: growth and properties. Surf Sci Nanotech 2005;3:131-140.

[254] Kohno H and Takeda S. Infusing metal into self-organized semiconductor nanonstructures. APL 2003;83(6):1202-1203.

[255] Kohno H and Takeda S. Non-gaussian fluctuation in the charge transport of Si nanochains. Nanotechnology, 2007;18:395706-395712.

[256] Cao C, He Y, Torras J, Deumens E, Trickey SB, and Cheng HP. Fracture, water, dissociation, and proton conduction in SiO_2 nanochains. J Chem Phys 2007;126:211101-211101.

[257] Wang Y, Nogami M, Shi J, Chen H, Ma G, and Tang S. Controlled surface-plasmon coupling in SiO_2-coated gold nanochains for tunable nonlinear optical properties. APL 2006;88:081110.

[258] Kohno H, Iwasaki T, and Takeda S. Metal-mediated growth of alternate semiconductor-insulator nanostructures. Solid State Communications 2000;116:591-594.

[259] Liu CM, Guo G, Wang RM, Deng Y, Xu HB, and Yang SH. Magnetic nanochains of metal formed by assembly of small nanopartilces. Chem Comm; 2004:2726-2727.

[260] Hong J and Wu RQ. Magnetic properties of Co nanochains. Phys Rev B 2004;70:060406(R).

[261] Pendelton A, Kundu S, and Liang H. Controlled synthesis of titanium nanochains using a template. J of Nanoparticle Research; 2008 (in press).

VITA

Alice Mae Pendleton was born in El Campo, Texas. She obtained a B.S. degree in biology, along with a B.S. degree in mechanical engineering, from Prairie View A&M University in Prairie View, Texas. She obtained a M.S. degree in Material Science at Rice University in 1983, and afterwards she immediately enrolled in their Ph.D. program in material Science, which she was unable to complete due to a catastrophic illness. After her three children were grown, she returned to Texas A&M University, and she received a Ph.D. in materials science and engineering in 2008.

Alice has much industrial experience with Monsanto as a project engineer. She worked at Dow Chemical as plant engineer before going to Rice University. After graduating from Rice University, she worked in Construction and Planning at Prairie View A&M University, and she taught a course, Computer Aided Design, within the Mechanical Engineering Department. While working on her Ph.D. at Texas A&M University, she was mainly involved in researching biofluids lubrication for artificial joints. She was able to utilize the tribometer, rheometer, profilometer, scanning electron microscope, and transmission electron microscope.

She is a member of several professional organizations such as SWE, ASME, NSBE and STLE. She has received NSF fellowship and she is a Sloan Scholar. In her spare time, she tutors students after school in reading and mathematics (up to pre-calculus) for Waller County. Alice Pendleton's contact information is Texas A&M University, Department of Mechanical Engineering, 3123 TAMU, College Station TX 77843-3123. Her email address is apendleton@tamu.